

การเตรียมเส้นใยซิลิกาที่มีหมู่อะมิโนโพรพิลสำหรับการดูดซับฟอรัมาลดีไฮด์ในน้ำ

นางสาวอัญชลี ท้วมบางไผ่

วิทยานิพนธ์นี้เป็นส่วนหนึ่งของการศึกษาตามหลักสูตรปริญญาวิทยาศาสตรมหาบัณฑิต

สาขาวิชาเคมี ภาควิชาเคมี

คณะวิทยาศาสตร์ จุฬาลงกรณ์มหาวิทยาลัย

ปีการศึกษา 2553

ลิขสิทธิ์ของจุฬาลงกรณ์มหาวิทยาลัย

PREPARATION OF AMINOPROPYL FUNCTIONALIZED SILICA FIBER FOR
ADSORPTION OF FORMALDEHYDE IN WATER

Miss Unchelee Thuambangphai

A Thesis Submitted in Partial Fulfillment of the Requirements
for the Degree of Master of Science Program in Chemistry

Department of Chemistry

Faculty of Science

Chulalongkorn University

Academic Year 2010

Copyright of Chulalongkorn University

Thesis Title PREPARATION OF AMINOPROPYL FUNCTIONALIZED
 SILICA FIBER FOR ADSORPTION OF
 FORMALDEHYDE IN WATER

By Miss Unchalee Thuambangphai

Field of Study Chemistry

Thesis Advisor Puttaruksa Varanusupakul, Ph.D.

Accepted by the Faculty of Science, Chulalongkorn University in
Partial Fulfillment of the Requirements for the Master's Degree

.....Dean of the Faculty of Science
(Professor Supot Hannongbua, Dr.rer.nat.)

THESIS COMMITTEE

..... Chairman
(Assistant Professor Suchada Chuanuwatanakul, Ph.D.)

..... Thesis Advisor
(Puttaruksa Varanusupakul, Ph.D.)

..... Examiner
(Assistant Professor Apichat Imyim, Ph.D.)

..... External Examiner
(Surapich Loykulnant, Ph.D.)

อัญชลี ท่วมบางไผ่ : การเตรียมเส้นใยซิลิกาที่มีหมู่อะมิโนโพรพิลสำหรับการดูดซับ
 พอร์มาลดีไฮด์ในน้ำ (PREPARATION OF AMINOPROPYL
 FUNCTIONALIZED SILICA FIBER FOR ADSORPTION OF
 FORMALDEHYDE IN WATER) อ.ที่ปรึกษาวิทยานิพนธ์หลัก : อ.ดร.พุทธรักษา
 วรานุศุภากุล, 89 หน้า.

เส้นใยซิลิกาสามารถใช้ในการดูดซับพอร์มาลดีไฮด์ซึ่งเป็นสารก่อมะเร็งในมนุษย์ ใน
 งานวิจัยนี้ได้เตรียมเส้นใยซิลิกาด้วยเทคนิคอิเล็กโตรสปินนิง ผ่านกระบวนการโซลเจล (sol-gel)
 โดยปัจจัยที่ทำการศึกษาซึ่งเกี่ยวข้องกับลักษณะเส้นใยที่เกิดขึ้นจากกระบวนการอิเล็กโตรสปินนิง
 นั้น ได้แก่ ระยะทางจากเข็มจนถึงฉากรองรับและศักย์ไฟฟ้า จากการทดลองพบว่า ระยะทางจาก
 เข็มจนถึงฉากรองรับและศักย์ไฟฟ้าที่เหมาะสมต่อการเตรียมเส้นใย คือ 10 เซนติเมตร และ 15
 กิโลโวลต์ ตามลำดับ โดยขนาดเส้นผ่านศูนย์กลางของเข็มที่ใช้มีค่า 0.8 มิลลิเมตร อัตราการไหล
 ของสารเท่ากับ 20 ไมโครลิตรต่อนาที ลักษณะเส้นใยที่ได้จากการวิเคราะห์ด้วยกล้องอิเล็กตรอน
 แบบส่องกราด พบว่าส่วนใหญ่ให้เส้นใยเรียบตรง สม่ำเสมอ ไม่เกิดปม มีขนาดเส้นผ่านศูนย์กลาง
 200-270 นาโนเมตร ในการเตรียมเส้นใยซิลิกาให้มีหมู่อะมิโนโพรพิล ได้ใช้ 3-
 aminopropyltriethoxysilane เป็นสารเติมให้เกิดหมู่อะมิโนโพรพิล โดยผลจากการวิเคราะห์
 ลักษณะพื้นผิว สัณฐานวิทยาและปริมาณหมู่ฟังก์ชันอะมิโนโพรพิลบนเส้นใยซิลิกาด้วยวิธี
 thermogravimetry, surface area analysis, elemental analysis และ Infrared spectroscopy
 พบว่าเส้นใยซิลิกาที่ผ่านการเติมหมู่ฟังก์ชันอะมิโนโพรพิล ให้ความแตกต่างทางโครงสร้าง พื้นผิว
 และหมู่ฟังก์ชันเมื่อเทียบกับเส้นใยซิลิกาที่ไม่ได้เติมหมู่ฟังก์ชันอย่างชัดเจน ทำให้สรุปได้ว่ามี
 หมู่อะมิโนโพรพิลเกิดขึ้นบนพื้นผิวของเส้นใยตามปริมาณของ 3-aminopropyltriethoxysilane ที่
 ใช้จริง นอกจากนั้นได้ทำการศึกษาปริมาณหมู่อะมิโนโพรพิล รวมทั้งระยะเวลาที่เหมาะสมต่อการ
 ดูดซับพอร์มาลดีไฮด์ในน้ำ ผลจากการทดลองพบว่า การใช้ 3-aminopropyltriethoxysilane
 ปริมาณ 0.15 โมลาร์ สำหรับการเติมหมู่ฟังก์ชันอะมิโนโพรพิล และดูดซับพอร์มาลดีไฮด์ในน้ำเป็น
 ระยะเวลา 3 ชั่วโมง เป็นภาวะเหมาะสมที่สุดต่อการดูดซับ สำหรับการชะออก พบว่าการใช้กรด
 ไฮโดรคลอริกหรือกรดซัลฟิวริกในการชะพอร์มาลดีไฮด์ออกจากเส้นใยซิลิกาด้วยความเข้มข้น
 เพียง 0.1 โมลาร์ เป็นระยะเวลา 15 นาที สามารถชะพอร์มาลดีไฮด์ออกจากเส้นใยซิลิกาได้มาก
 ที่สุด

ภาควิชา.....เคมี..... ลายมือชื่อนิสิต.....
 สาขาวิชา.....เคมี..... ลายมือชื่อ อ.ที่ปรึกษาวิทยานิพนธ์หลัก.....
 ปีการศึกษา.....2553.....

507 26043 23 : MAJOR CHEMISTRY

KEYWORDS : SILICA FIBER / ELECTROSPINNING/ ADSORPTION/
FORMALDEHYDE

UNCHALEE THUAMBANGPHAI : PREPARATION OF
AMINOPROPYL FUNCTIONALIZED SILICA FIBER FOR
ADSORPTION OF FORMALDEHYDE IN WATER. THESIS ADVISOR
: PUTTARUKSA VARANUSUPAKUL, Ph.D., 89 pp.

The silica fibers can be applied for adsorption of formaldehyde which had been classified as a carcinogen in human. In this study, silica fibers were fabricated by electrospinning technique via sol-gel process. Many factors that affect the morphology of electrospun fibers including the distance between syringe needle and collection screen, as well as electric potential were studied. The optimized distance and electric potential were 10 cm and 15 kV, respectively. The diameter of the needle of 0.8 mm and flow rate 20 μ L/min were selected for the optimum condition for preparation of electrospun silica fibers. The Scanning Electron Microscope (SEM) images illustrated that most of silica fibers were smooth and straight with diameters in the range of 200-270 nm. For preparation of functionalized silica fibers, 3-aminopropyltriethoxysilane (APTES) was used for aminopropyl functionalization. Characterization with thermogravimetry, surface area analysis, elemental analysis and Infrared spectroscopy showed the clear difference between aminopropyl functionalized on electrospun fibrous silica mats and non-functionalized electrospun silica fibers. It could conclude that aminopropyl group could be successfully grafted on electrospun silica fibers. Using 0.15 M APTES for functionalization of silica fibers with APTES and subsequent adsorption of formaldehyde in water for 3 hours were the optimum method. In the part of elution, the optimum condition was using hydrochloric acid or sulfuric acid with concentration of 0.1 M and elution for 15 minutes.

Department.....Chemistry..... Student's Signature

Field of Study.....Chemistry..... Advisor's Signature

Academic Year2010.....

ACKNOWLEDGEMENTS

My research can be successfully completed with helpfulness and support from my respectful advisor, Dr. Puttaruksa Varanusupakul who has been giving useful advisements for solving many problems through my experiment. With her informal relationship, insightful discussions and suggestions make me pleasure and be joyous to my progress laboratory. So, I would like to express my sincere appreciation for them with my great thankfulness. Additionally, my thesis committees, videlicet, Assistant Professor Dr. Suchada Chuanuwatanakul, Assistant Professor Dr. Apichat Imyim, and Dr. Surapich Loykulnant, who give me any opinions and valuable suggestions for my work and devote their valuable time for my thesis defense examination. And I was grateful to members of EARU (Environmental Analysis Research Unit) in 1201 and 1204 for generousness about all equipments including hood and distillation equipment. Furthermore, with kindness, encouragement and lovely friendship of all members of Chromatography and Separation Research Unit, and my all classmates in Master degree of Analytical chemistry, particularly in 1205/1207 laboratory gave me spirituality and helpfulness for doing my work until my research was completely finished. And not forgotten to utter mention, I would like to thank my beloved family, especially my lovely mother who has been giving me many supports and great willingness for further my lab until success comes.

Ultimately, my thanks are also extended to The 90th anniversary of Chulalongkorn University Fund (Ratchadaphiseksomphot Endowment Fund), and Center of Petroleum, Petrochemicals and Advanced Materials, Chulalongkorn University for grateful acknowledgement financial supports my research work.

CONTENTS

	Page
ABSTRACT (IN THAI).....	iv
ABSTRACT (IN ENGLISH).....	v
ACKNOWLEDGEMENTS.....	vi
CONTENTS.....	vii
LIST OF TABLES.....	xi
LIST OF SCHEMES.....	xii
LIST OF FIGURES.....	xiii
LIST OF ABBREVIATIONS AND SYMBOLS.....	xv
 CHAPTER	
I. INTRODUCTION.....	1
1.1 Statement of purpose.....	1
1.2 Scopes of this research.....	4
1.3 The benefit of this research.....	4
 II. THEORY.....	 5
2.1 Silica.....	5
2.1.1 Properties of silica.....	5
2.1.2 Preparation of silica via sol-gel process.....	11
2.1.2.1 Hydrolysis.....	12
2.1.2.2 Polycondensation.....	14
2.1.2.3 Gelation.....	15
2.1.2.4 Aging.....	16
2.1.2.5 Drying (dehydration or chemicastabilization).....	16
2.1.2.6 Densification.....	16
2.1.3 Modification of silica or polysiloxane.....	17
2.1.3.1 Modification through impregnation.....	17
2.1.3.2 Modification through covalent bond.....	17
2.1.3.2.1 Immobilizaion of silane reagent (grafting).....	17
2.1.3.2.2 Silica surface modification with sol gel route.....	18

	Page
2.2 Electrospinning.....	20
2.2.1 History of electrospinning.....	20
2.2.2 Process of electrospinning.....	21
2.2.2.1 Fluid charging.....	22
2.2.2.2 Generation of droplet.....	23
2.2.2.3 Formation of cone jet (Taylor cone).....	24
2.2.2.4 Thinning jet formation.....	24
2.2.2.5 Elongation of the straight fragment.....	25
2.2.2.6 Whipping instability of jet.....	25
2.2.2.7 Solidification of nanofiber.....	27
2.2.3 Parameters of electrospinning process.....	28
2.2.3.1 Solution parameters of electrospinning.....	28
2.2.3.1.1 Concentration.....	28
2.2.3.1.2 Molecular weight.....	28
2.2.3.1.3 Viscosity.....	29
2.2.3.1.4 Surface tension.....	29
2.2.3.1.5 Conductivity/Surface charge density.....	29
2.2.3.2 Processing parameters of electrospinning.....	30
2.2.3.2.1 Applied voltage.....	30
2.2.3.2.2 Feed rate or Flow rate.....	30
2.2.3.2.3 Collectors types.....	31
2.2.3.2.4 Tip to collector distance.....	31
2.2.3.2.5 Diameter of needle.....	31
2.3 Adsorption.....	32
2.3.1 Types of adsorption.....	32
2.3.1.1 Physisorption.....	32
2.3.1.2 Chemisorption.....	33
2.3.2 Classification of adsorption isotherm.....	33
2.3.2.1 Type I isotherm.....	34
2.3.2.2 Type II isotherm.....	34
2.3.2.3 Type III isotherm.....	34

	Page
2.3.2.4 Type IV isotherm.....	35
2.3.2.5 Type V isotherm.....	35
2.3.2.6 Type VI isotherm.....	36
2.3.3 Adsorption isotherm models.....	36
2.3.3.1 Langmuir isotherm.....	36
2.3.3.2 Brunauer-Emmett-Teller (BET) adsorption isotherm.....	38
2.3.3.3 Freundlich and Küster isotherm.....	41
III. EXPERIMENTAL.....	42
3.1 Materials.....	42
3.1.1 Preparation of silica sol by electrospinning process.....	42
3.1.2 Functionalization of electrospun fibrous silica mats.....	42
3.1.3 Adsorption and elution of formaldehyde in water.....	42
3.1.4 Standardization of formaldehyde solution.....	42
3.1.5 Determination of formaldehyde by spectrophotometry method....	43
3.2 Methodolgy.....	43
3.2.1 Preparation of silica fibers.....	43
3.2.2 Preparation of the functionalized fibrous silica mats with 3-aminopropyltriethoxysilane (APTES).....	44
3.2.3 Characterization of functionalized electrospun silica fibers.....	44
3.2.3.1 Fourier-Transform Infrared Spectrophotometry (FT-IR)	44
3.2.3.2 Scanning Electron Microscopy (SEM).....	45
3.2.3.3 Thermogravimetric Analysis (TGA).....	45
3.2.3.4 Surface area analysis	45
3.2.3.5 Elemental analysis (EA).....	46
3.2.4 Study of efficiency of functionalized silica fiber.....	46
3.2.4.1 Adsorption of formaldehyde solution.....	46
3.2.4.2 Elution of formaldehyde solution.....	47
IV. RESULTS AND DISCUSSION.....	48
4.1 Morphology of electrospun fibrous silica mats.....	48
4.1.1 Electrospun fibrous silica mats before functionalization.....	48

	Page
4.1.2 Electrospun silica fibers after functionalization with 3-aminopropyltriethoxysilane (APTES).....	52
4.2 Characterization of non-functionalized and functionalized electrospun fibrous silica mat with APTES.....	57
4.2.1 Fourier-transform Infrared Spectrophotometry (FT-IR).....	57
4.2.2 Elemental analysis (EA).....	60
4.2.3 Thermogravimetric Analysis (TGA).....	61
4.2.4 Surface area analysis.....	63
4.3 Adsorption of formaldehyde in water.....	69
4.4 Elution of adsorbed formaldehyde in water.....	74
V. CONCLUSIONS	77
5.1 Conclusion.....	77
5.2 Suggestion of future work.....	78
REFERENCES	79
APPENDIX	87
VITA	89

LIST OF TABLES

Table		Page
2.1	The different forms of crystalline phase of silica.....	6
4.1	Fiber formation and average diameter of fibers.....	50
4.2	Average diameter of fibers functionalized with APTES various concentrations (nm).....	55
4.3	The IR characteristic peaks of non-functionalization silica fibers (-SiO ₂), functionalized silica fibers with APTES (-SiC ₃ H ₆ NH ₂) and functionalized silica fibers with APTES after formaldehyde adsorption (-Si-C ₃ H ₆ N=CH ₂).....	59
4.4	The percentage of average amount of some elements from elemental analyzer.....	60
4.5	Grafting percentage and loading capacity of aminopropyl group into eletrospun fibrous silica mats.....	62
4.6	Variables from BET-Plots of non-functionalized and functionalized silica fibers.....	66
4.7	Pore characteristics and surface area of electrospun fibrous silica mats.....	67
4.8	Adsorbed quantity of formaldehyde with functionalized fibrous silica mats at various APTES concentrations and several adsorption times.....	71

LIST OF SCHEMES

Scheme	Page
2.1 Hydrolysis and polymerization of silicon chloride.....	9
2.3 Mechanism of acid catalyzed hydrolysis.....	13
2.4 Mechanism of base catalyzed hydrolysis.....	14
2.5 Condensation of (a) silanol-silanol group, and (b) silanol-alkoxysilane.....	14
2.6 A polycondensation of siloxane compound.....	15
2.7 Grafting process of APTS on silica gel surface.....	18
2.8 Grafting process of DETA on silica surface with chloropropyl silica	18
2.9 Examples of functionalized silica via sol-gel process, a) amine and b) thiol functionalized polysiloxane ligands by hydrolytic condensation and c) multi step of functionalization of 3-aminopropyltrimethylsilane (APTMS) and followed by co-polymerization of TEOS.....	19
4.1 Grafting process of aminopropyl group on silica.....	54
4.2 Self-polymerization of APTES	55
4.3 Imine formation.....	59
4.4 Reaction between functionalized silica fibers with APTES and formaldehyde (imine formation).....	69
4.5 The mechanism of reaction between APTES and formaldehyde (imine formation) where R represents $-C_3H_6Si(OC_2H_5)_3$	70
4.6 Chemical reaction between silica and formaldehyde.....	72
4.7 Hydration reaction of aldehyde to form germinal diol.....	72
4.8 Instability reaction of aminopropyl group on modified silica.....	73
4.9 The regeneration of formaldehyde (the elution formaldehyde from aminopropyl functionalized silica).....	75
A-1 Derivatization of formaldehyde to form 3,5-diacetyl-1,4-dihydroxyltoluidine.....	88

LIST OF FIGURES

Figure		Page
2.1	The three structures of silanol groups.....	10
2.2	Schematics of set up of electrospinning apparatus : (a) a typical vertical set up, (b) a typical horizontal set up.....	21
2.3	Taylor cone formations under increase of applied electric field till both surface tension and electric force in equilibrium (State III).....	24
2.4	Whipping region of a typical electrospinning jet : (a) unperturbed cylindrical fluid element, (b) varicose (s=0) instability, (c) whipping (s=1) (so called “bending” or “kink”) instability, (d) splitting (s=2) instability.....	26
2.5	Whipping fluid jet formation.....	27
2.6	Types of physisorption isotherms.....	34
2.7	The characteristic of graphical form of the Langmuir isotherm.....	37
2.8	BET-plot of any sample.....	40
2.9	An example of BET isotherm.....	40
2.10	An example of Freundlich sorption isotherm.....	41
4.1	SEM micrographs of electrospun silica fibers obtained from 9 conditions by changing the electric fields and distance between syringe needle and collection screen. Original magnifications 7,500x	49
4.2	Average diameters of electrospun fibers at various electric potentials and distances between the needle and the collection screen.....	51
4.3	SEM images of electrospun silica fibers mats functionalized with (a) 0.10 M (b) 0.15 M, (c) 0.25 M (d) 0.50 M APTES, (e) 0.75 M, and (f) 1.0 M APTES. Original magnifications 1,500 x (big images) and 7500 x (small images).....	53
4.4	The structure of 3-aminopropyltriethoxysilane (APTES).....	54

Figure	Page
4.5 The IR spectrum of electrospun fibrous silica mats of (a) non-functionalization, (b) aminopropyl functionalization with APTES and (c) aminopropyl functionalization after formaldehyde adsorption	57
4.6 Thermogravimetric analysis (TGA) curves of electrospun silica fibers mat with (a) non-functionalization, and functionalization with (b) 0. 1M (c) 0.5 M (d) 1.0 M 3-aminopropyltriethoxysilane (APTES).....	61
4.7 Nitrogen adsorption isotherms of non-functionalized fibrous silica mat, and fibrous silica mat functionalized fibrous silica mats with 0, 0.15 M, 0.50 M, and 1.00 M APTES, respectively.....	64
4.8 BET-Plots of non-functionalized silica fibers, silica fibers functionalized with 0.15 M APTES, 0.50M APTES, and 1.00 M APTES, respectively.....	65
4.9 Pore size distribution of (a) non-functionalized and functionalized fibrous silica mats with (b) 0.15 M, (c) 0.50 M, (d) 1.00 M APTES, respectively.....	68
4.10 The relationship of APTES concentrations and adsorbed formaldehyde with functionalized silica fibers at various adsorption times.....	70
4.11 The relation between the percentage of elution and the various concentrations of HCl and H ₂ SO ₄ : 0.1, 0.3, 0.5, 1.0 M at fixed time of 15 minutes.....	75
4.12 The relationship between elution time and the percentage of elution at the fixed concentration acid at 1.0 M.....	76

LIST OF ABBREVIATIONS AND SYMBOLS

cm	Centimeter
cm ²	Square centimeter
°C	Degree Celcius
K	Kelvin
kV	Kilovolt
g	Gram
mg	Milligram
mg/m ³	Milligram per cubic meter
M	Molar concentration
MPa	Mega Pascal
min	Minute
mL	Milliliter
μL	Microliter
mm	Millimeter
nm	Nanometer
ppm	Part per million
ppb	Part per billion
RSD	Relative standard deviation
S/m	Siemens per meter
%w/v	Percentage weight by volume

CHAPTER I

INTRODUCTION

1.1 Statement of purpose

Formaldehyde is one type of aldehyde compound, which can naturally be in gas or aqueous phase. 37-50 %w/v formaldehyde solution is called formalin. Generally, the physical properties are colorless, soluble in water, and polar solvents. Moreover, formaldehyde has a strongly pungent odor, highly flammable and quickly decomposes to form formic acid and carbon monoxide in air [1]. For the chemical properties, it can react with strong oxidizers, alkalis and acids, phenols and urea. Many formaldehyde applications include antiseptic in medical treatment and medicine-based industries such as forensics, pathology laboratories, hospitals, etc. In addition, formaldehyde is widely used in the manufacture of formaldehyde-based resins, plastics, adhesives and a film processing, textile treatments, leather tanning and a wide range of personal care and consumer products [2].

Formaldehyde in ambient air is released from consumer product such as building materials and home furniture that its average concentrations reported in U.S. urban were between 11-20 parts per billion (ppb). The level of formaldehyde in home building was reported in the range of 0.10-3.68 parts per million (ppm) [3]. However, higher levels have been found in new materials more than older conventional homes. The main sources of releasing this gas appeared to be automobile exhaust emissions, plants and incinerators while formaldehyde may also present in food due to result of contamination in nature.

At present, formaldehyde is proposed to be a hazardous compound because of high toxicity. Low levels of formaldehyde (< 0.1 ppm; < 0.12 mg/m³) can be adsorbed in the gastrointestinal and respiratory tracts and metabolism in body. Formaldehyde also induces allergenic contact urticaria and dermatitis in humans. Higher level (0.1-0.3 ppm; 0.12-0.36 mg/m³ and > 0.3 ppm; > 0.36 mg/m³) can cause a fluid of lungs,

throat spasms, skin burns, eye irritation and asthma attack whose symptoms include wheezing, cough or tightness and leading to shortness of breath [4]. Recently, the National Occupational Health and Safety Commission (NOHSC), the United States Environmental Protection Agency (U.S. EPA) and the International Agency for Research on Cancer (IRAC) which is part of the World Health Organization (WHO) classified this substance as a probable human carcinogen owing to its high toxicity [1-6]. WHO had defined an exposure standard at 80 ppb more than 30 minutes, while Occupational Safety and Health Administration (OSHA) allowed an exposure limit at 750 ppb and dangerous level for health limit at 20 ppm [7] At present, the standard value of formaldehyde in water source must not be more than 0.1 ppm [5].

Mostly, the method for formaldehyde removal is adsorption using special solid called adsorbent. This process is extensively used for formaldehyde removal because of simplicity and low cost. Many kinds of adsorbent are often used for this removal including activated carbon from many natural sources such as coffee residuals [8, 9], heat-treated rice husks [10], and karamatsu (*Larix leptolepis*) bark [11]. Furthermore, activated carbon containing amino groups had been used for adsorption of formaldehyde because amino group was responsible for selective adsorption and reactivity [12], and activated carbon fibers were used as the fine adsorbent for the substance because of high surface area and porosity [13].

Addition to activated carbons, silica gel had been widely used for formaldehyde adsorption. Particularly, modified silica gel with amine group on its surface area is mostly used as adsorbent. For example, Yang et al. [14] studied an efficiency of formaldehyde and acetaldehyde adsorption by using non-modified silica gel and modified silica gel with aminopropyl group. The results showed that a capable of formaldehyde adsorption with aminopropylsilylated silica gel is more effectively than non-modified silica which was a more effective adsorbent for acetaldehyde. Seung et al. [15] modified silica gel particles with three types of amine groups by using three kinds of the silane coupling agents including 3-aminopropyl-triethoxysilane (APTES), *n*-(2-aminoethyl)-3-aminopropyl-trimethoxysilane (AEAP) and 3-(2-(2-aminoethylamino) ethylamino) propyltri-methoxysilane (AEEA). Silica gel with amine group can absorb formaldehyde more effectively than non-modified silica gel and APTES was the most suitable coupling agent for functionalization on silica for

formaldehyde adsorption. For other studies, such as the research's Jadkar and coworkers [16], they used Cu_2C_2 -silica gel as formaldehyde adsorbent and added metal oxide for increasing of capability of formaldehyde adsorption. Owing to high efficiency of modified surface area of silica gel to amine group for adsorption, this is an alternative approach for my study.

Generally, silica gel for adsorption is synthesized via sol-gel process to form silica particles. However, silica can be prepared to be fibers form with electrospinning process [17-20] which is a simple technique and prevalent used for producing polymer fibers by using an electrostatically driven jet of polymer melt. Diameters of electrospun silica fibers are very small in the range of micro to nanometer; therefore, the surface area of obtained fiber is very high effecting to the high ratio of surface to volume (or mass) of the fibers. Furthermore, the efficiency of adsorption by using electrospun silica fibers mats as adsorbent may be higher than using silica particles as adsorbent or equal one.

Apart from adsorption, many researchers determined the quantities of formaldehyde after adsorption; for example, Kiba et al. [21] determined the amount of nano-molar levels of formaldehyde in drinking water. They eluted adsorbed formaldehyde in polyallylamine beads with 1 M HCl before injecting into flow-injection system for examination of formaldehyde recovery which was $> 96\%$ with RSD of $\leq 3.0\%$. The same researchers group [22] examined an efficiency of adsorption by using polyallylamine bead as an adsorbent for formaldehyde and acetaldehyde and then adsorbed formaldehyde and acetaldehyde were eluted with sulfuric acid before derivatization with 2,4-dinitrophenylhydrazine for detection with HPLC in the next step.

On account of a good efficiency of amine functionalized silica for formaldehyde adsorption and many advantages of silica fibers over silica particles; for example, they are easily prepared by electrospinning which have a few equipments and large surface area to volume ratio affecting to adsorb more efficiently and more comfortable than silica particles for handle, application of continuous flow work in industry, and good capability in a wide range of advanced applications: filtration, sensor, wound healing, catalyst and enzyme carrier, etc [23]. The modification of amine group on silica fibers preparation is novel and interested alternation of

adsorbent. Moreover, it is very useful for solving the environmental and health problem, particular formaldehyde, a human carcinogen, which can be finely adsorbed with this adsorbent.

1.2 Scopes of this research

- 1.2.1 Preparation of fibrous silica mats via eletrospinning process.
- 1.2.2 Functionalization of silica fibers with 3-aminopropyltriethoxysilane to grafting amine group on silica surface for using as adsorbent.
- 1.2.3 Study the efficiency of these adsorbents in formaldehyde adsorption and elution by determination of formaldehyde with standard method of ASTM and UV-visible spectrophotometry.

1.3 The benefit of this research

Alternative adsorbent for adsorption of formaldehyde in water

CHAPTER II

THEORY

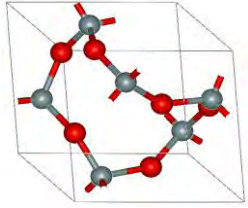
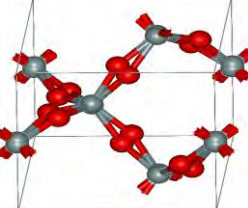
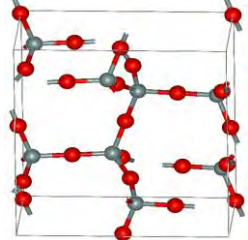
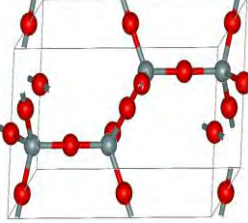
2.1 Silica

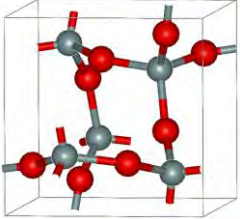
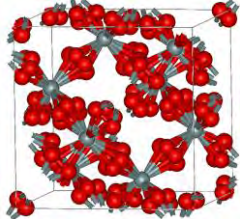
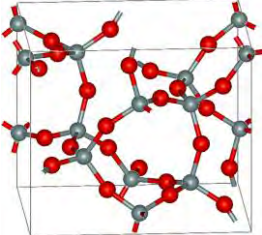
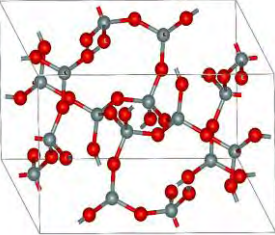
2.1.1 Properties of silica

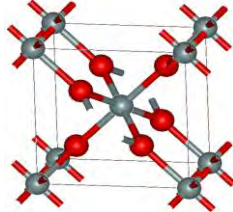
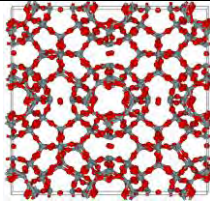
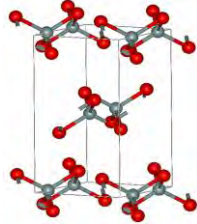
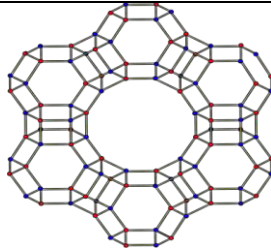
Silica or silicon dioxide (SiO_2) is the most common substance which can be easily found on earth. The structure of silica is tetrahedron which consists of four oxygen atoms surrounding on a central silicon atom [24]. Most common forms found in natural are quartzite, sandstone, and sand silica. Several forms of silica: crystal, glass, aerogel, pyrogenic silica (fumed silica) and colloidal silica are manufactured for many applications. Primarily, silica is a raw material to produce window glass, beverage bottles, and drinking glassware. Additionally, it is used for a primary raw material in whiteware ceramics production such as porcelain, stoneware, and earthenware. It is also used as an additive in the food production such as an agent for powered food and water absorber in hygroscopic applications.

Generally, silica can occur in the two phases which are amorphous and crystalline phase [25]. Although both phases have identical atomic ratios of silica and oxygen, their structures were different. Amorphous form (vitreous silica, glassy solid) as silica glass, silica atoms form with a continuous disorder network. As crystalline phase, including quartz, tridymite, and cristobalite, forms a well-ordered lattice and continued over a large network. Both silica structures can be transformed into stable form; for example, amorphous phase can be changed into crystalline forms: tridymite and cristobalite when it is heated at temperature of 870°C and 1470°C , respectively [26]. In addition to high temperature, pressure and chemical environment are main parameters for this transformation.

Table 2.1 The different forms of crystalline phase of silica [27]

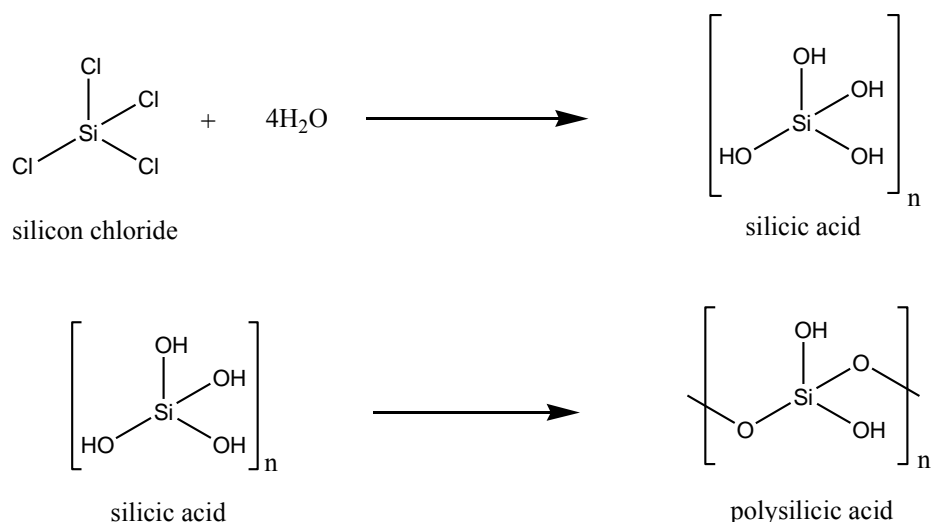
Form	Crystal symmetry	Details	Structure
α -quartz	Rhombohedral (trigonal) [28]	individual single crystals optically active because of helical chains; α -quartz converts to β -quartz at 846 K	
β -quartz	Hexagonal [29]	closely related to α -quartz (with an Si-O-Si angle of 155°) and optically active; β -quartz converts to β -tridymite at 1140 K	
α -tridymite	Orthorhombic	metastable form under normal pressure	
β -tridymite	Hexagonal	closely related to α -tridymite; β -tridymite converts to β -cristobalite at 2010 K	

Form	Crystal symmetry	Details	Structure
α -cristobalite	Tetragonal [30]	Meta stable form under normal pressure	
β -cristobalite	Cubic [31]	closely related to α -cristobalite; melts at 1978 K	
Keatite	Tetragonal	Si_5O_{10} , Si_4O_{14} , Si_8O_{16} rings; synthesized from amorphous silica and alkali at 600–900 K and 40–400MPa	
Coesite	Monoclinic [32]	Si_4O_8 and Si_8O_{16} rings; 900K and 3000–3500 MPa	

Form	Crystal symmetry	Details	Structure
Stishovite	Tetragonal [33]	rutile like with 6-fold coordinated Si; 7500–8500 MPa	
Melanophlogite	Cubic [34] or tetragonal [35]	Si_5O_{10} , Si_6O_{12} rings; mineral always found with hydrocarbons in interstitial spaces-a clathrasil [36]	
Fibrous (Poststishovite)	Orthorhombic	Like SiS_2 consisting of edge sharing chains	
Faujasite	Cubic [37]	Sodalite cages connected by hexagonal prism. 12-membered ring pore opening	

For Table 2.1 shows the twelve different forms of silica crystal structure. One silica structure can transform to the other which is more stable depending on ambient temperature and pressure. Mostly, silica structures such as β -cristobalite, Keatite, Coesite, Stishovite and Faujasite, are complex and strong, so they are melted at high temperature and pressure. Additionally, silica structure of transformation can take place to form more condensed structure when pressure exchanges such as stishovite and coesite because of the intense compression of the atoms during their formation.

Ordinarily, silica is polymer of silicic acid or polysilicic acid which consists of interconnected SiO_4 tetrahedron. Silicic acid is produced from hydrolysis of silicon tetrachloride (SiCl_4) and can polymerize to form polysilicic acid condensing to cross-linked gel [24].



Scheme 2.1 Hydrolysis and polymerization of silicon chloride

For the outer surface of silica, atomic force microscopy (AFM) is a technique of image measurement, which uses a specific probe for surface scanning. In general, the surface of silica can be both siloxane group ($\equiv\text{Si-O-Si}\equiv$) and silanol groups ($\equiv\text{Si-OH}$) [38].

In view of free silanol group, it was discovered in 1936 by Kiselev [38], who studied the physical and chemical methods for calculation of silanol number on surface. Silanol group was weak acid and its concentration on surface after

operation at 423 K was 4.5-8.0 group nm^{-2} depending on kind of silica [39, 40]. Silanol group on silica surface can be divided into three kinds including isolated silanol (free silanol), vicinal silanol (bridged silanol), and geminal silanol (silanediols) [41]. For isolated silanol, three bonds of silica molecule are connected with other silica to form bulk structure and one bond is connected to a hydroxyl group (-OH). Vicinal silanol has two silanol groups which attach to each silicon atom forming in tetrahedral structure. And geminal silanol connects to one silicon atom in the structure. Structures of those silanol groups were shown in Fig 2.2

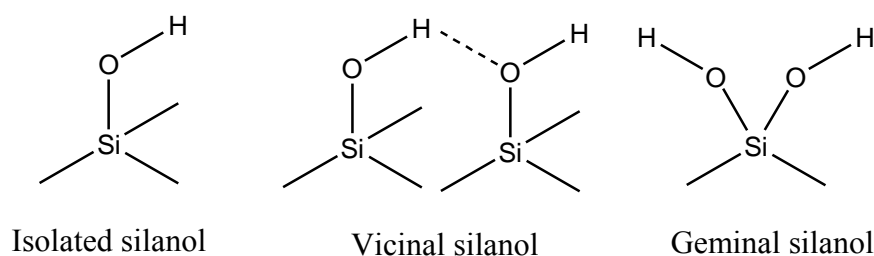


Figure 2.1 The three structures of silanol groups [25,38]

Ong and coworkers [42] reported that pK_a values of silanol at interface of silica and water were both 4.9, and 8.5. At lower pK_a values, silanol groups were expected to be isolated silanol groups which did not form hydrogen bonding with any side chains because their hydroxyl groups could easily break when compared with the other silanol groups. As silanol with higher pK_a value may be silanols that directly connected via hydrogen bonding or bridged with water molecules.

In many cases, the surface properties of amorphous silica depend on the presence of silanol groups. A sufficient concentration, surface of silica shows such hydrophilic property. The hydroxyl group (-OH) anchored at surface can interact to OH groups of other molecules with a hydrogen bond. The removal of these hydroxyl groups from silica surface results in decreasing of these interactions, surface of silica becomes more and more hydrophobic properties.

2.1.2 Preparation of silica via sol-gel process

The method for preparation inorganic materials, ceramics and organic-inorganic hybrid proceeding via polymerization and polycondensation reaching to solid phase network formation at low temperature between 25 and 80°C, is a sol-gel process. This method was interested and widely manipulated with several procedures such as incorporation, entrapment, encapsulation with various materials such as organic substances, inorganic substances, biomolecules, microorganism, tissue and indicators, etc.

The process was developed to solve many problems from the general preparation of those materials with high temperature solid state reactions. This was firstly processed since the mid-1800s (1845) by Ebelman and Graham who studied the synthesis of silica gel via hydrolysis under acidic condition with tetraethyl orthosilicate but this work is a little industrial interest. Next, many researches of gel synthesis were studied; for example, in 1950s-1960s, Roy and co-workers [43, 44] prepared homogeneous colloidal gels with sol-gel method and synthesized a large number of novel ceramic oxide compositions such as Aluminium (Al), Silicon (Si), Titanium (Ti), Zirconium (Zr), etc. Meanwhile, Iler [45] also studied on chemistry of silica, and then his silica product was successfully developed to become commercial silica powder as Dupont's colloidal Ludox spheres. Afterwards, Stober spherical silica powders were yielded from extending of Iler's work by Stober and co-workers [46]. They used ammonium as catalyst in hydrolysis reaction of tetraethylorthosilicate (TEOS) for controlling the size and morphology of their prepared silica powders. Furthermore, the controlled morphologies and size of colloidal powders with transition metal oxide (TiO_2 , $\alpha\text{-Fe}_2\text{O}_3$, Fe_3O_4 , BaTiO_3), hydroxides ($\text{Al}(\text{OH})_3$, $\text{Cr}(\text{OH})_3$), carbonates ($\text{Cd}(\text{OH})\text{CO}_3$, $\text{Ce}_2\text{O}(\text{CO}_3)_2$), sulfides (ZnS , CdS), metals ($\text{Fe}(\text{III})$, Ni , Co) and mixed composites (Ni , Co , Sr), sulfides ((Zn, CdS) , (Pb, CdS)) and coated particles (Fe_3O_4 with $\text{Al}(\text{OH})_3$, or $\text{Cr}(\text{OH})_3$), etc. were studied. In addition, glass and polycrystalline ceramic fibers such as $\text{TiO}_2\text{-SiO}_2$, $\text{ZrO}_2\text{-SiO}_2$ glass fibers, and $3\text{Al}_2\text{O}_3\cdot 2\text{SiO}_2$ fibers, etc. were prepared and developed to become commercial products in the current.

The sol-gel process involves a colloidal suspension or dispersions of colloidal particles (solids with diameters of 1-100 nm [47]) in a liquid, which is so-called sol, gradually evolves towards formation of a gel-like a globally connected solid matrix including a liquid and solid phase. In part of gel, gel was rigid network with pore diameters in submicron and its average polymeric chain length is more than micron. Gel can be divided into four forms by Flory [48] viz, (1) well-ordered lamellar structure, (2) covalent polymeric network which is completely disordered, (3) polymer networks formed via physical aggregation, predominantly disordered, and (4) particular disordered structure.

Procedure of sol-gel process

The processing steps which involve in preparation of silica gel with sol-gel method comprise six following steps:

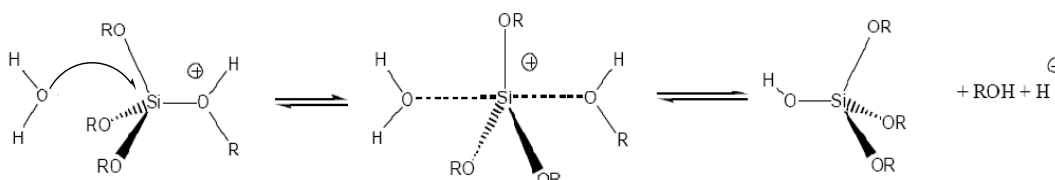
2.1.2.1 Hydrolysis

The first step for synthesis of silica including particles, fiber or monolith is hydrolysis. Precursor commonly used in this process is metal alkoxide, which is one kind of organometallic compounds that are organic compounds consisting of metal atom in molecules. Its general formula is $M(OR)_n$ where M is metal, R is alkyl group including aliphatic, cyclic, and aromatic compounds. Metal alkoxide widespread for this process is alkoxy silane ($Si(OR)_4$) with R= methyl, (-CH₃), ethyl (-C₂H₅), and propyl (-C₃H₇), etc. They are often used in sol-gel chemistry as precursor in synthesis of silica, especially alkoxy silanes with low molecular weight such as tetramethyl orthosilicate (TMOS): $Si(OCH_3)_4$, tetraethyl orthosilicate (TEOS): $Si(OC_2H_5)_4$ because alkoxide group (-OR) in structure can easily leave to form network of polysiloxane (Si-O-Si), and these typical silanes could be insoluble in water, but can homogeneously soluble in system.

This process needs to be catalyzed with two kinds of catalysts including acid and base.

(i) Acidic catalyst hydrolysis

Hydrolysis procedure with acidic catalyst was often used for sol-gel process. Mechanism of acidic catalyzed hydrolysis was given as:



Scheme 2.3 Mechanism of acid catalyzed hydrolysis [25]

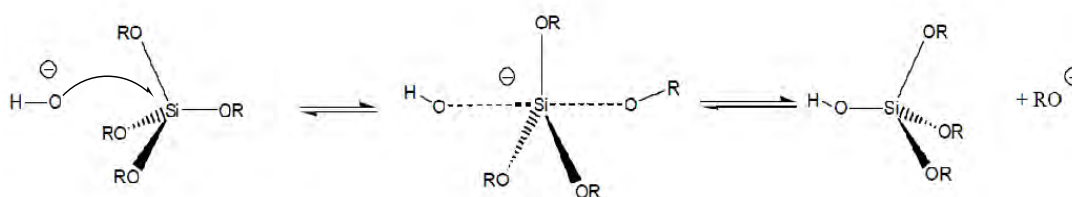
From mechanism shown in Scheme 2.3, the proton from acid is attracted by oxygen atom of alkoxy group (-OR) to form positive charge on this oxygen atom. Then, H₂O molecule attacks to silicon atom to form a positive charge on it. This step is called a transition state. ROH molecule will leave from this intermediate and Si(OH)(OR)₃ product will be continuously formed.

Hydrochloric acid not only was the most frequently used, but also other acids such as acetic acid (CH₃COOH), sulfuric acid (H₂SO₄), phosphoric acid (H₃PO₄), etc. have been used as catalyst [25]. However, the resulting gel did not depend on any kind of acidic catalyst.

Under chemical condition for acid catalyzed sols, hydrolysis is comparatively faster than condensation reaction and a more branches opened chain of polysiloxane network is continuously produced. Polymer formation can be drawn or spun from sol to fibers, thin film into surface coatings, etc.

(ii) Basic catalyst

Hydroxyl ion (OH⁻) from basic catalyst is nucleophile which attacks to silicon atom to form negative charge on silicon atom in transition state. Alkoxide ion (OR⁻) will leave from this intermediate to produce Si(OH)(OR)₃. Basic catalyst extensively used is ammonia [49-51]. Mechanism of reaction is preceded as follows.

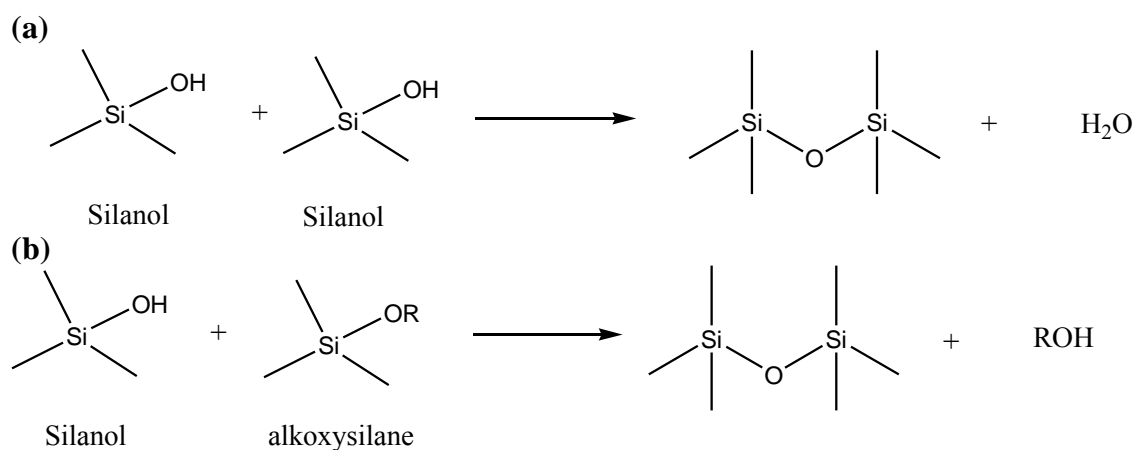


Scheme 2.4 Mechanism of base catalyzed hydrolysis [24]

In this condition, reaction of condensation was faster than hydrolysis and a high degree of cross-linkages with large molecular weight of siloxane are formed. The obtained particles will continuously grow to be colloidal particles (colloids).

2.1.2.2 Polycondensation

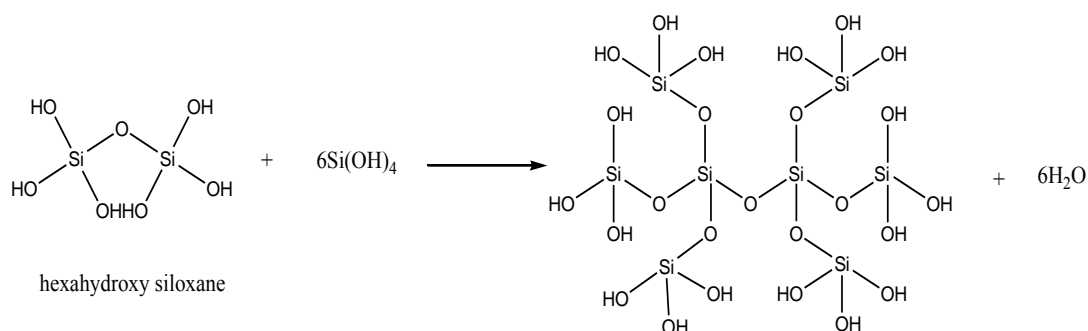
This procedure can divide into two types including condensation of silanol group and silanol group, and silanol group and alkoxy silane. The reactions of both condensations were shown in Scheme 2.5.



Scheme 2.5 Condensations of (a) silanol-silanol group, and (b) silanol-alkoxy silane

After condensation, additional of -Si-OH can link to form a large molecular-weight polymer via polycondensation reaction and ultimately forms a silica

network and byproducts such as water and organic solvent remained in the pores of this great interconnected linkage.



Scheme 2.6 A polycondensation of siloxane compound [52]

In the procedure of condensation reactions, a large amount of Si-O bonds sufficiently interconnect to form sol or colloidal particles which have diameters in submicron level. Both the size and cross-linking or density of sol particles rely on the pH of solution in system and ratio between concentration of H_2O and $\text{Si}(\text{OR})_4$ ($[\text{H}_2\text{O}]/[\text{Si}(\text{OR})_4]$).

2.1.2.3 Gelation

When the linkage of sol particles increases until it leads to gel-point, the sol becomes gel, more viscous and loses its liquidity and forms a three dimensional network. This process also involves the previous step, polycondensation affecting to the morphology of particles because of time dependent control of viscosity from sol to gel.

2.1.2.4 Aging

This process can be called syneresis which regards to preserve the resulting gel for a period time such as hours to days or months, etc. During aging of gel process, bonds formation, by product i.e., water and alcohol production (hydrolysis) and additional polycondensation (cross-linking) effecting on occurrence of pore shrinkage (decreasing porosity) happen at the same time. All mentioned results effect on structure and properties of this gel as the function of time. If aging time increases, the strength of gel will also increase.

2.1.2.5 Drying (Dehydration or chemical stabilization)

Organic solvent and moisture remaining in the gel are evaporated from pore in cross-linking network and pore volume of solid slightly shrinks. In case of diameters of pores after drying are less than 20 nm, gel can crack and break because of large internal pressure gradients in pores of gel from the different rate of liquid removal in large and small pores. To prevent this fracture, the addition of surfactants such as Triton-X is proposed [53]. Subsequent thermal treatment or low temperature sintering is about 500-600°C. The obtained gel may be performed a higher density product and a chemically stable micro or ultraporous solid.

2.1.2.6 Densification

Sintering at high temperatures resulted in elimination of pores and a density of the product becomes more increasingly. The densification temperature depends on the dimensions of the pore cross-linkage, the interconnections of those pores, and surface area. And temperature for densification of alkoxide gels is about 1000-1700°C depending upon the radii of the pores and the surface area [52].

2.1.3 Modification of silica or polysiloxane

In general, the modification of surface of silica involves many processes that affect to change in chemical properties of the silica surface. Physical treatment (thermal or hydrothermal) is a method which can change ratio of silanol and siloxane concentration of silica surface. Meanwhile, chemical treatment is a process which leads to change the chemical characteristics of silica surface. The most convenient method for chemical modification on silica surface is simple immobilization or fixing the functional group on surface by electrostatic or adsorption or hydrogen bond formation or other interactions.

2.1.3.1 Modification through impregnation

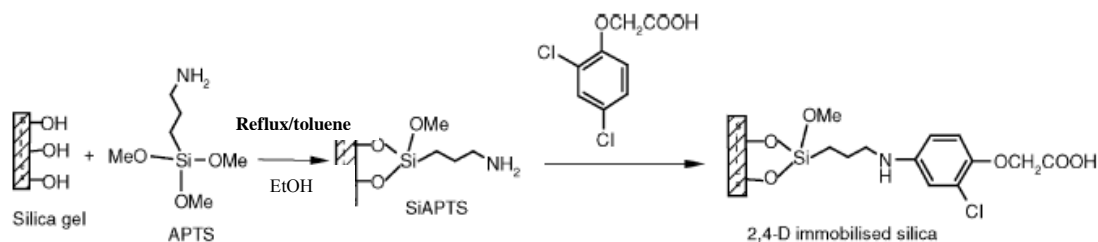
Impregnation of modifier solutions or covalent binding, so called covalent grafting of chelating molecules to the silica surface is a simple method for functionalized silica surface with physical interaction between the modifier and silica solid support. For example, the immobilization onto a silica gel with 8-hydroxyquinoline (8-HQ) by stirring with the activated silica for metal extraction [54], using 2,4-dinitrophenylhydrazine (2,4-DNPH) impregnated on silica gel surface for adsorption of formaldehyde in air as hydrazone complex [55]. And the immobilization of ECB-T (indicator) as solid phase extractor onto silica surface for determination of Zn(II), Mg(II) and Ca(II) ions [56].

2.1.3.2 Modification through covalent bond

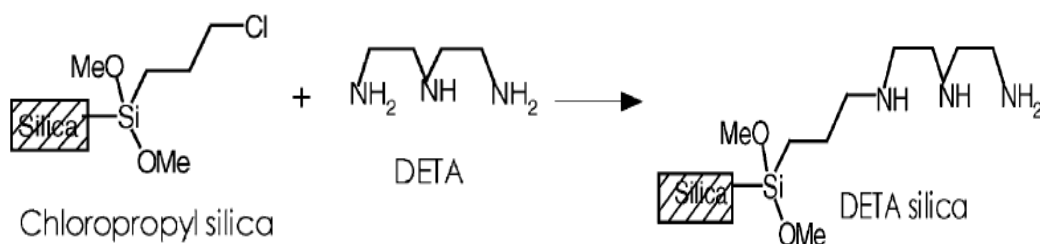
2.1.3.2.1 Immobilization of silane reagent (grafting)

Immobilization of organic functional groups on silica surface has been widely manipulated for production of many different types modified silica. Generally, both organic reagent and molecules containing an organic functional group are attached initial silica chains, and the products gradually extend these chains. Therefore, the organic chelating groups containing the desired functional groups were

formed and enhanced to specific adsorption such as the functionalized acidic surface of silica with 3-aminopropyltrimethoxysilane (APTS) and following 2,4-dichlorophenoxyacetic acid (2,4-D) [57], and the treatment of chloropropyl silica surface with diethylenetriamine (DETA) [58].



Scheme 2.7 Grafting process of 2,4-D on silica gel surface [38]



Scheme 2.8 Grafting process of DETA on silica surface with chloropropyl silica [38]

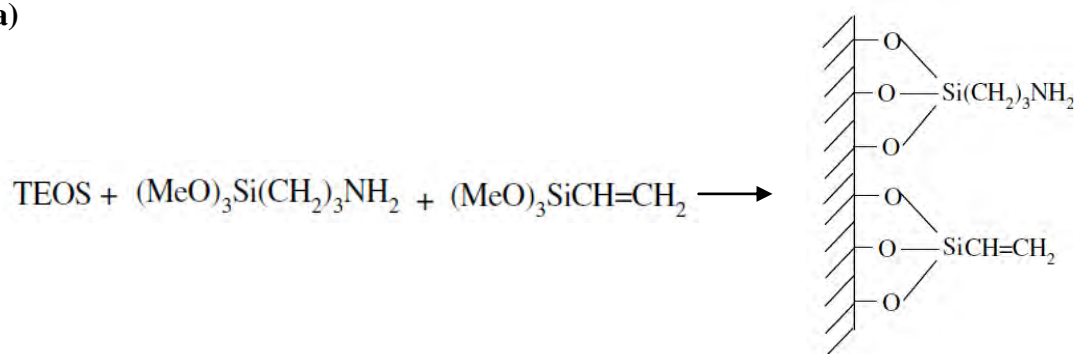
2.1.3.2.2 Silica surface modification with sol gel route

Sol-gel process has been used for synthesis of organically modified silica (ormosil). The most common procedure involved hydrolyzing a tetraalkoxysilane compound in an alcohol and water, the product were formed silica having alkoxy group and hydroxy groups connected to the silicon atom at the surface and following mixing with an organosilicon compound.

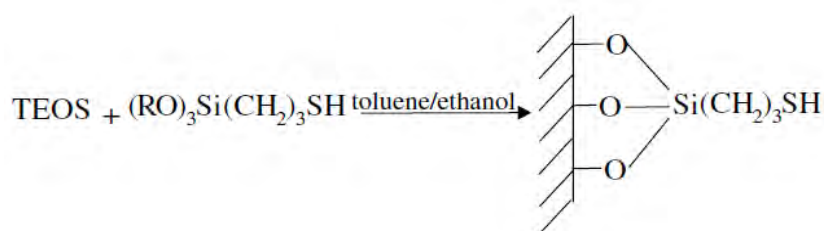
In fact, there are two categories for modification of silica or immobilized polysiloxane ligand system [59]. First one is the preparation of modified polysiloxane chain with substance consists of desired functional group (complexing ligand) by hydrolytic condensation and then continuous condensation by

precursor such as tetramethoxysilane (TMOS), tetraethylorthosilicate (TEOS). For this method, amount of complexing ligand or functional group can take place with high quantity which is more than the second one. The second category is hydrolysis and condensation between siloxane chains and continuously functionalized with immobilized ligand or functional group. The functionalized group must be stable and difficult to leave from siloxane. This method can be called the post-treatment of polysiloxane or post synthesis functionalization.

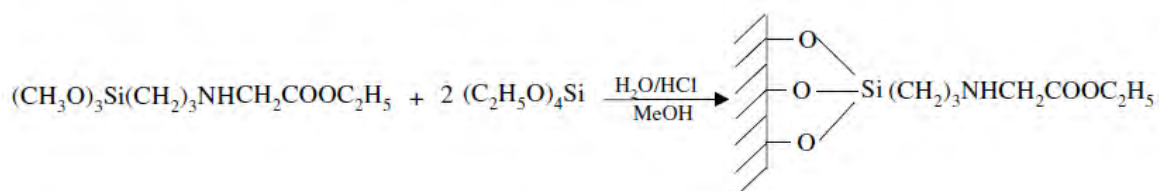
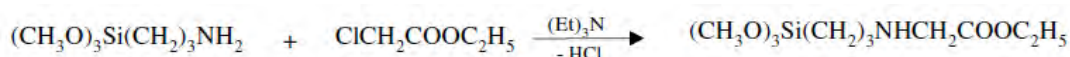
a)



b)



c)



Scheme 2.9 Examples of functionalized silica via sol-gel process, a) amine and b) thiol functionalized polysiloxane ligands by hydrolytic condensation and c) multi step of functionalization of 3-aminopropyltrimethylsilane (APTMS) and followed by copolymerization of TEOS [25]

2.2 Electrospinning

Electrospinning process is extensive technique for fiber production by using electrical forces to form fibers with diameters of micro or nanometers ranges. Mostly, obtained fibers have high surface area and several small pores as compared with general fibers from other techniques. Since many advantages of electrospun nanofibers such as small diameters, an extremely high surface-to-volume ratio, ability to modify their properties including sizes and shapes and functionalization, high tunable porosity with pore interconnection, etc. With these advantages, these fibers are applied in many applications including chemical and optical sensor, electrode materials, protective clothing, biomedical, pharmaceutical, healthcare, tissue engineering scaffolds, filtration, and catalyst, etc.

2.2.1 History of electrospinning

Electrospinning was originated in 1897 by Rayleigh and was studied in detail of electrospaying by Zeleny [60] in 1914. After that, this subject in term of electrospinning was first patented in 1934 by Formhals. For the first patent, it described in using a voltage of 57 kV for electrospinning of cellulose acetate with acetone and monomethyl ether of ethylene glycol as solvents and continuous published a series of them which was detailed in experiment setup preparation of polymer fibers with electrostatic force [61] since 1938, 1939 and 1940. In 1952, Vonnegut and Newbauer [62] devised an apparatus consisting of electrical atomization and produced streams whose diameter of electrified droplet of 0.1 mm. Subsequently, in 1955, there was study on the dispersion of liquids of aerosols with high voltages and in 1966, Simons [63] was patented an experimental setup for fabrication of ultra thin non-woven fibers with light weight using different conditions of electrical spinning. Next, in 1969, Taylor [64] published the appearance of polymer droplet at the end of a capillary when an electric field applied. He found that the droplet changes its shape into a cone (called “Taylor cone”) and subsequently determinate that a cone angle of 98.6 degrees was optimum composition for balancing the surface tension with electrostatic forces by varying different viscous fluids [65].

In 1971, Baumgarten [66] began to study on the solution and processing parameters such as viscosity of solution, flow rate, and applied voltage, etc. about properties of electrospun fibers. He built an apparatus for production of acrylic fibers from polyacrylonitrile and dimethylformamide (DMSO) as solvent. His results were concluded that fiber diameter directly related to viscosity of solution (higher viscosities giving bigger diameters). Moreover, fiber diameter does not only decrease with increasing applied electric field, but also diameter would increase when further increasing applied potential after reaching a minimum. His electrospun fibers had diameters between 0.05-1.1 μm . After that, about a decade, Larrondo and Mandley [67] electrospun fiber of polyethylene and polypropylene melts for investigation of fibers structural properties from polymer melts. They discovered diameters of polymer melts had larger than those of solution and inversely depended on temperature of melting. And then this process based on electrospinning was widely grown in many research institutes, universities and some companies including eSpin Technologies, NanoTechnics, KATO Tech and Donaldson Company and Freudenberg for various applications in recent years.

2.2.2 Process of electrospinning

Electrospinning is a technique of spinning which is approached using electrostatic forces to produce small fibers from melt polymer or polymer solution. At present, there are two typical experimental setups for electrospinning including a vertical and a horizontal apparatus which are shown in Figure 2.2

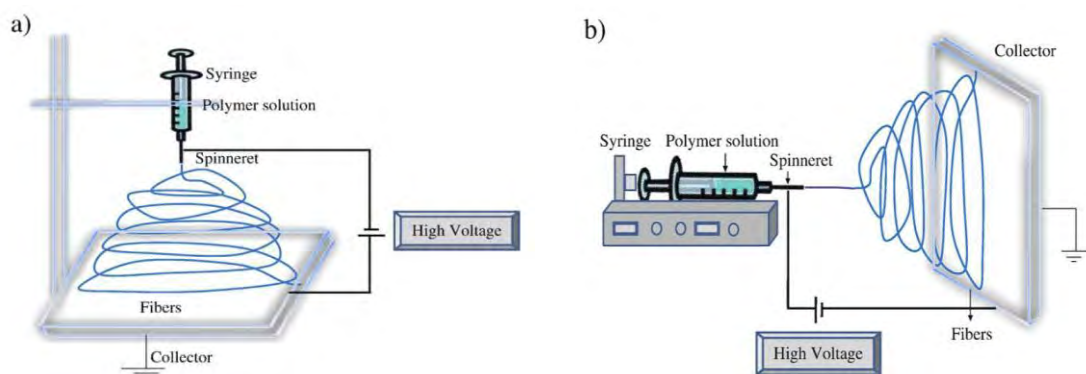


Figure 2.2 Schematics of set up of electrospinning apparatus [68] :

(a) a typical vertical set up, (b) a typical horizontal set up

For the main components of electrospinning apparatus, there are three equipments for this system including

- a high voltage power supply with positive or negative polarity
- a spinnerate such as pipette tip, a capillary with metal needle
- a grounded collecting plate such as a metal screen, stationary plate, and rotation drum or mandrel

In the electrospinning process comprising of several operational components [69]:

- i) a charging of the fluid
- ii) a formation of the cone-jet (Taylor cone)
- iii) a thinning of the jet in the presence of an electric field
- iv) an instability of the formed jet
- v) the collection of the jet or its solidified fibers on the appropriate target

2.2.2.1 Fluid charging

With the nature of the fluid and polarity of the electrical potential, both free electrons and ions or ion pairs were produced in the form of charge conductors in the fluid. However, the charge induction involved impurities in solution. The ions or ion pairs generation can generate from an electrical double layer. For charging of fluid in electrospinning, it was limited with applied electric field. Generally, the inductive charging suitable for fluids was conductivities of 0.01 S/m, but in the case of non-conductive fluids including polymer melts and hydrocarbons, their inductive charges may be directly forced to the fluid in technique of electrostatic thrusters. The examples of this method were presented by Kim and Turnbull in electrospaying [70] and Kelly who produced fibers by electrospinning with a charge injection apparatus which was first developed for atomization of fuel.

2.2.2.2 Generation of droplet

After charging of fluid which is the first step of electrospinning, the polymer melt or solution flows with either controlling of syringe pump or influence of gravity and will form a droplet when the fluid reaches to the end of needle. Supposing that the liquid surface tension is γ , the gravity force is F_G , the droplet radius is r_0 , and the internal radius of needle is R , the relation of all these factors can be presented as:

$$r_0 = (3R \gamma / 2 \rho g)^{1/3}$$

where ρ is the liquid density and g is the gravitational constant

In the presence of the high voltage, the electric force, F_E will force contrarily to the force of needle surface likely as $F_\gamma = F_E + F_G$, and the radius of droplet at the end of needle subsequently decreases as r ($r < r_0$). The F_E , and r values [48] in the electrospinning process can be calculated from:

$$F_E = (4\epsilon\pi V^2) / [\ln(4L/R)^2]$$

$$r = \{(3/2\rho g)[R_\gamma - (2\epsilon V^2)/(\ln(4L/R))]\}^{1/3}$$

where V is a positive electric potential, distance of tip to collector is L , and ϵ is the permittivity of the medium (e.g. air).[71]

The process of droplet generation begins with applied electric potential to the droplet; the electrical conduction in it is produced. When the positive charge is applied to the needle, it will proceed to the droplet surface. On the other hand, the negative charge collects in the internal droplet for balancing charge, the field in the droplet is zero. This charge separation can induce a force which is countered by surface tension in the droplet and the stability of the charged droplet at needle tip needs the internal surface tension force to outdo the outer repulsion force

which accumulates on the drop surface. For the maximum number of charges that a droplet can grasp previous to the electrical forces overwhelms the surface tension of droplet can be formulated, and the value had been first discovered by Rayleigh.

2.2.2.3 Formation of cone-jet (Taylor cone)

Under applied electrical potential, the spherical pendant droplet at needle tip will become hemispherical and continuously convert to a conical shape which so called Taylor's cone. Taylor [64] studied on the equilibrium of the cone formation in condition consisting of electric potential and surface tension. The result was shown that the half angle of was 49.3° . For the cone, it can be produced by using the critical potential, V_c for applying to drop at the needle tip, a needle whose length and external radius are h and r , respectively.

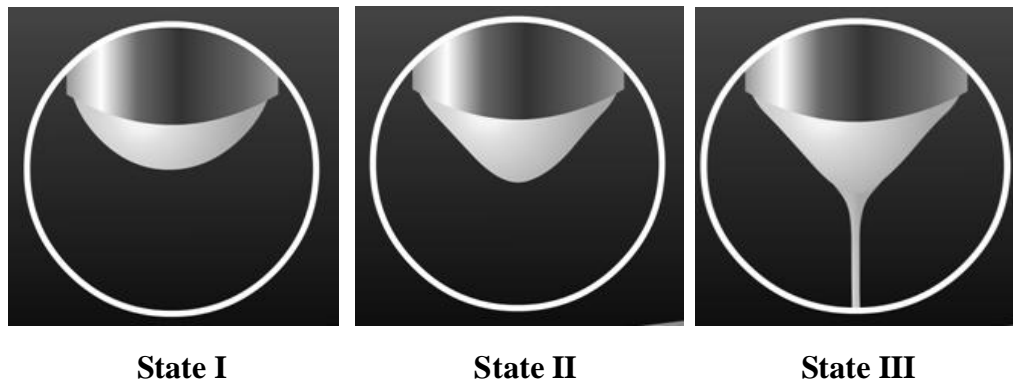


Figure 2.3 Taylor cone formations under increase of applied electric field till both surface tension and electric force in equilibrium (State III)

2.2.2.4 Thinning jet formation

The state which is apart from the conical base is called jet. This formation is caused by accelerating the polymer melt or polymer solution to stretch to be straight segment. In addition, the jet usually occurs at the layer surface of the resulting cone. However, using concentrated solution affects abundant complexity of polymer chains, and a coulombic repulsion is insufficiently generated to burst it. The

surface area needed to improve for charging on the jet surface during the fibers formation. The addition of surface area is originally generated from the Taylor cone for adjustment of surface charges. And it subsequently partly spouts toward into the collection screen because of the generation of its surface shear force from the electrical potential difference between the conical base and the Taylor's cone tip.

2.2.2.5 Elongation of the straight fragment

The elongation step of the jet occurs when applied electric field exceeds the critical voltage (V_c). This process begins with the columbic repulsion of the charges on the jet surface in axial formation, and then this jet stretches toward the collection screen. The velocity of jet relates to the distant away from the Taylor cone. With increasing of the distant, the several diverse of velocity directly are gained. Then the size of jet diameter rapidly shrinks owing to the extension and evaporation of solvent. After acceleration of applied voltage, the jet decreases in diameter to form a thin one and the surface area unit per unit mass of jet increases, but the charge on jet surface per unit area reduces. In addition, the evaporation of solvent directly affects to the increase of the surface charges per unit area due to the extension of surface area.

2.2.2.6 Whipping instability of jet

During the passage of jet to the collector, the straight jet segment is unstable, flexible and undulating movement. Bending of jet increases surface area and tends to decrease the charges density. The whipping jet formation is caused by the competition of varieties of instability modes [72, 73] such as Raleigh instability, axis-symmetric instability, and bending mode instability. The mode of instability depends on the electric potential, with high potential favoring this whipping instability. With the components of electrostatic repulsive forces, this jet subsequently whips within a cone and symmetrically forms at its straight axis.

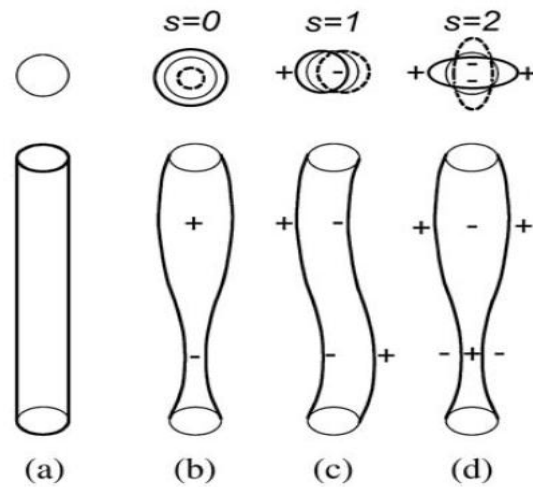


Figure 2.4 Whipping region of a typical electrospinning jet : (a) unperturbed cylindrical fluid element, (b) varicose ($s=0$) instability, (c) whipping ($s=1$) (so called “bending” or “kink”) instability, (d) splitting ($s=2$) instability.[69]

Reneker [74] describes that diameters of spiral will increase when the jet rapidly spouts and the cone-shaped envelope of unstable jet is produced by the rapid symmetric movement of a single jet. The straight jet is held, the additional volume of envelope leads to the greater diameter of spiral through the perimeter of this loops. The increasing rate in surface area during the whipping instability and solvent evaporation rate, lead to reduce the diameter jet. The parameters of the charge density, viscosity, and surface tension forces against the stretching of the others create complexity of the instability.

The variety of forces on the whipping charged jet during electrospinning includes

1. Gravitational force (F_G) which goes toward the collector in a vertical apparatus depends on density of solution.

$$F_G = \rho \pi r^2 g$$

where ρ is the density of the liquid and g is the acceleration due to gravity.

2. The electrostatic force (F_E) which forms jet extension and drives toward the grounded collector relates to the applied electrical potential and material properties.
3. Coulombic repulsion (F_C) depends on the characteristics of the polymer and solvent and contributes whipping motion and instability.
4. Viscoelastic forces which resist the elongation of the jet, this depends on the molecular weight of polymer, the polymer type, and solvent
5. Surface tension forces work the same as viscoelastic force. It depends on the kinds of solvent, polymer and additives
6. Frictional forces at the jet surface and the enclosing air or gas

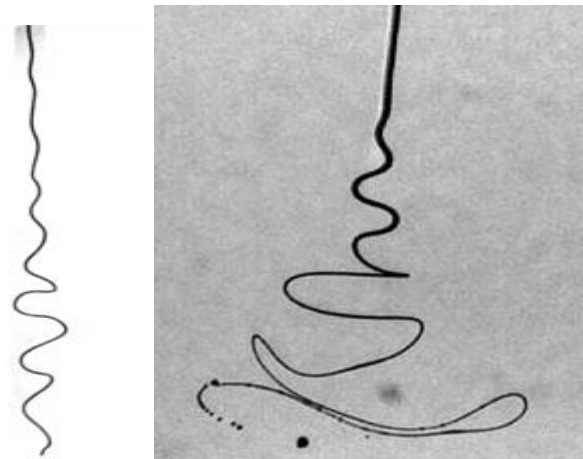


Figure 2.5 Whipping fluid jet formation [69]

2.2.2.7 Solidification of nanofiber

During the rate of evaporation of solvent happens with increasing rate in whipping, a mass base on the jet increases. A solvent with having high vapor pressure affects to the deformation of a viscose stretching jet in early stage of the whipping instability and resulted in the thick nanofibers formation. The important factor of controlling the fiber diameter is solvent volatility. And the appropriate selection of solvents and process parameters, extremely fine fibers can be electrospun in the electrospinning process.

2.2.3 Parameters of electrospinning process

The main factors which affect electrospinning process can be classified into three parts: solution parameters, process parameters, ambient parameters. These parameters have an effect on the morphology and diameters of the electrospun fibers.

2.2.3.1 Solution parameters of electrospinning

2.2.3.1.1 Concentration

At low solution concentration, both beads and the fibers is altogether formed. On the other hand, at the high concentration, the appearance of beads can convert from globular to pivot form and a final fiber with larger diameters is created, it caused by the increasing of viscosity resistance within solution and the inability to uphold the solution flow at the end of the needle tip. In addition, both solution surface tension and viscosity are the major factors for studying on concentration range that continuous fiber can be generated [68].

2.2.3.1.2 Molecular weight

One of the main roles that affect to rheological (i.e. surface tension, viscosity) and electrical properties (i.e. conductivity and dielectric strength) is molecular weight [75]. In general, at a low molecular weight polymer solution, it often produces beads on fibers more than only fibers formation, as a high molecular weight solution, the larger diameter of fibers are formed. In point of view, chain entanglement is a main role which related to molecular weight parameter. At large molecular weight can sufficiently maintain the number of entanglements on the polymeric chains in solution to create an identity jet in electrospinning process and decrease a bead formation on fibers caused by surface tension.

2.2.3.1.3 Viscosity

Both of size of fibers and the appearance of polymer fibers are resulted from the role of solution viscosity. With low viscosity, a continuous fiber is not able to produced due to role of surface tension, as high viscosity, it is difficult to discharge the jet from solution and often evinces a longer stress relaxation times which inhibits the cracking of jet during spinning process. Additionally, increasing of the viscosity or concentration of polymer solution produces larger more unvaried diameter fibers. There were reported that the maximum viscosities for electrospinning is in the range of 1-215 poise [66]. Three parameters such as viscosity, polymer concentration and molecular weight of polymer are related to each other.

2.2.3.1.4 Surface tension

Another parameter which plays an important role in the process is surface tension. Ordinarily, with high surface tension of solution prohibits the process of spinning owing to an unsteadiness of the jet and the production of sprayed droplets [76, 77]. Whereas the lower surface tension of solution is not always suitable for electrospinning; however, the obtained electrospun fibers from this has no bead formation.

2.2.3.1.5 Conductivity/Surface charge density

Mostly, polymers have conductive properties which depend on kind of polymer, solvent for polymer solution preparation, and the availability of ionisable salts. When the electrical conductivity in solution increases, the diameters of the electrospun fibers will decrease. Additionally, the highly conductive solutions are unstable and produce an extremely bending to form a broad diameter range under applied high electric fields, as with low conductivity of the solution, the stretching of the jet with the force of electric potential is not enough for

the uniform and beads formation. Besides an increase in conductivity of the solution by adding ionic salts such as NaH_2PO_4 , K_2HPO_4 , NaCl , the fibers are increasingly formed with uniformity and the reduction of beads formation on fibers is observed.

2.2.3.2 Processing parameters of electrospinning

2.2.3.2.1 Applied voltage

A typical important parameter of electrospinning is the applied electric potential or voltage to polymer solution. At the optimum applied field can generate the electrospun fibers. Operating this parameter for electrospinning gives the results of the sizes of the obtained fibers including the smaller and larger ones. In case of an increase in the applied voltage also increasingly effects on the electrostatic repulsive force on the jet, results in a favorable thinner fiber formation. Moreover, a larger stretching of the solution caused by the greater coulombic force in the jet leads to a decrease in diameter of fiber, and solvent can also rapidly vaporize, and probably form beads on the fibers. Although the applied voltage relates to a diameter fiber, the concentration of polymer solution and distant between needle tip and the collector are considerably parameters effecting on the size of fibers.

2.2.3.2.2 Feed rate or Flow rate

The influence of feed rate or flow rate of polymer can observably affect the velocity of the jet fluid, transformation rate of material, and morphology of the obtained fibers. An enough time for solvent evaporation with a low feed rate is an objective for electrospinning process as a result of no bead formation on fibers and the decrease in diameter of fibers. On the contrary, with a high flow rate applied in the process of electrospinning, the resulting fiber is formed with the opposite outcome.

2.2.3.2.3 Collectors types

The collector, the main equipment for electrospinning process, is a conductive matter where the electrospun fibers are deposited. Mostly, Aluminium foil is a material used as a collection screen, but it may not be comfortable for removal of the obtained fibers or is not suitable for manifold applications. Apart from aluminium foil, conductive paper, conductive cloth, wire mesh [78], pin [79], parallel bar [80], rotating rod, rotating wheel [81], liquid non solvent such as methanol coagulation bath, are several alternatives in place of the foil.

2.2.3.2.4 Tip to collector distance

Another parameter for controlling the diameter and shape of the electrospun fibers is the distance between the needle tip and the collection screen. There are some researchers reported that a minimum distance is needed because the fibers required a minimum distance to be produced with an adequate time for drying before approaching to the collection; otherwise the beads are formed on the fibers. It has been also reported that the thinner fibers are formed at the closer distance. An influential physical characteristic of the electrospun fibers is aridity from solvent for dissolving the polymer. Consequently, the optimum distance between a tip and collector is needed for solvent evaporation.

2.2.3.2.5 Diameter of needle

The diameter of needle tip effects on the characteristic of the electrospun fibers. With a small needle diameter, the clogging and bead formation are reduced and the flatter fibers are formed because the acceleration of jet decreases, and this allows more time for the solution to be stretched and elongated before it was collected on the screen, but the surface tension of droplet at the end of needle tip increases. As with a large diameter of needle, the characteristic of the fibers is big and has often bead formation.

2.3 Adsorption

The enrichment or depletion of one or more components in an interfacial layer or the actual distribution of a component between the interfacial layer and the bulk phases is called adsorption (or sorption). The substrate in the adsorbed state is defined as an adsorbate (sorbate) while that present in one or other of the bulk phases and capable of being adsorbed may define as the adsorptive (sorptive). The adsorptive and adsorbate may be chemically different species. The adsorption can occur at the interface between a fluid phase and a solid called adsorbent (sorbent) or gas/liquid interfaces or liquid/liquid interfaces. And in absorption, the structure of the adsorbent and/or the chemical nature of the adsorptive may be modified. Most of adsorbents widely used are activated carbon, silica gel, zeolite, polymer bead, etc. Generally, adsorption is process for cleaning up hazardous waste or purified drinking water.

2.3.1 Types of adsorption

Adsorption process is generally classified as physisorption and chemisorptions.

2.3.1.1 Physisorption

Physisorption is a physical separation process that the adsorbed substance does not chemically react to another phase and adsorbs on the surface of another phase with van der Waals forces from induced dipole-dipole interaction. This phenomenon can occur in any solid/fluid system depending on geometrical or electronic properties of the both of adsorbent and adsorbate. In addition, this process does not involve activation energy. The adsorption process slowly forms at ambient temperature with equilibrium between the adsorbent and adsorbate. In solid/gas system, the extent of the physical adsorption increases with increase in gas pressure and often decreases with increasing temperature. Molecules of adsorbate can excessively adsorb on surface which is multilayer adsorption or filling in micro or mesopores.

2.3.1.2 Chemisorption

Chemisorption is a chemical separation process that occurs at the surface and characterized by chemical specificity. The interaction between the adsorbate and adsorbent surface involves electronic bonds such as ionic or covalent bond, so adsorbate molecules usually occupy certain adsorption sites on the surface and be form only one layer of adsorbents molecules (monolayer adsorption). In general, chemical reaction of adsorption can be exothermic or endothermic reaction and usually involves an activated energy.

2.3.2 Classification of adsorption isotherm

Adsorption isotherm is the relation between the quantity adsorbed and the composition of the bulk phase or the partial pressure in the gas phase under equilibrium conditions at constant temperature. It is displayed in graphical form with the amount adsorbed (preferably n^a in mol g^{-1}) plotted against the equilibrium relative pressure (p/p^0) where p^0 is the saturation pressure of the pure adsorptive at the temperature of the measurement or against p when the temperature is over than the critical temperature of the adsorptive. [82]

$$n^a = f\left(\frac{P}{P^0}\right)_{T, gas, solid}$$

The characteristics of the isotherms feature involve the nature of the gas-solid interaction and the surface area and porosity of the adsorbent which are classified to three sizes including micropores which have widths less than 2 nm, mesopores which have widths in the range 2-50 nm, and macropores which have widths more than 50 nm and are less importance in the physisorption of nitrogen.

The majority of isotherms can be divided into the six types shown Figure 2.6

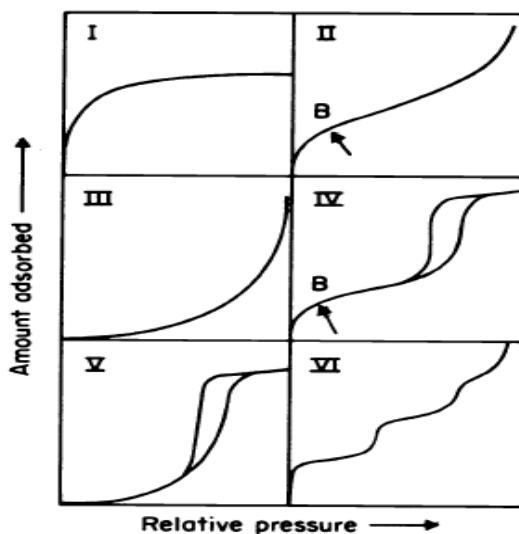


Figure 2.6 Types of physisorption isotherm [83]

2.3.2.1 Type I isotherm

Type I isotherm can be defined by microporous solids which have relative small external surface. The limiting uptake can access into micropore volume more than internal surface area. The examples of this isotherm are the adsorption of nitrogen on surface of activated carbon at 77 K, adsorption of ammonia on surface of charcoal at 273 K.

2.3.2.2 Type II isotherm

The Type II isotherm is the common form of a non-porous or macroporous adsorbent. It stands for monolayer-multilayer adsorption. Point B in Type II isotherm of Figure 2.14 divides into 2 stages of the stage of monolayer coverage and multilayer adsorption, respectively.

2.3.2.3 Type III isotherm

The III isotherm is the typical for vapor adsorption which indicates the characteristic of adsorbate-adsorbent interactions. Generally, this isotherm

associates with non-porous and microporous adsorbent. For example, adsorption of water vapor molecules on carbon surface in which the primary adsorption sites are oxygen based, and bromine or iodine adsorption at 79°C on silica gel.

2.3.2.4 Type IV isotherm

The type IV isotherm has hysteresis loop which is associated with capillary condensation form in mesopores, and the limiting uptake over a range of high p/p^0 . The initial part of Type IV isotherm is attributed to monolayer adsorption because it has the same path of Type II isotherm which is characteristic of non-porous form of adsorbent and followed by multilayer adsorption. The characteristics of this isotherm relate to the mono-multilayer adsorption. Examples of this Type IV include the adsorption of benzene on iron oxide (Fe_2O_3) at 500°C or the adsorption of benzene on silica gel at the same temperature.

2.3.2.5 Type V isotherm

This isotherm is similar to isotherm of Type III but has hysteresis loop which indicated a weak interaction between adsorbent and adsorbate with microporous or mesoporous form and appeared the capillary condensation of adsorbent in these pores. Example of this isotherm is the adsorption of water vapor on activated carbon.

2.3.2.6 Type VI isotherm

The isotherm shows the many steps where involves the system of adsorption and ambient temperature. It is a hypothetical isotherm which details in the complete formation of monomolecules layer with strong interaction before advancement to a next layer. This characteristic of isotherm represents the stepwise multilayer adsorption on non-porous surface. The step height indicates the monolayer capacity of each adsorbed layer and in two or three adsorbed layers, the capacity

reaches to a constant. For example of this isotherm is the adsorption of argon or krypton gas on graphitized carbon blacks at liquid nitrogen temperature.

2.3.3 Adsorption isotherm models

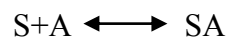
Four isotherm models including Langmuir, Brunauer-Emmett-Teller (BET), Freundlich, indicates the characteristic of adsorption equilibrium.

2.3.3.1 Langmuir isotherm

Irving Langmuir (1916) studied an isotherm for adsorption of gases on solids or the partition between gas phase and adsorbed species as function of applied pressure. His isotherm proposed from a kinetic mechanism is based on four hypotheses:

- 1) The surface of the adsorbent is uniform, all the adsorption sites are equal.
- 2) Adsorbed molecules must not interact with other molecules.
- 3) Adsorption process must occur through the same mechanism.
- 4) Only monolayer is formed at the maximum adsorption and adsorbate molecules do not cover on the surface.

For thermodynamics, the adsorption process between gas phase molecules (A) and vacant (S) and occupied surface sites (SA) can be showed as



Assuming there is a fix number of surface sites on the surface and equilibrium constant (K) is given as

$$K = \frac{[SA]}{[S][A]}$$

$[SA]$ is a parameter that relates to the surface coverage of adsorbed molecules, i.e. proportional to θ

$[S]$ is a parameter which represents the number of vacant sites, i.e. proportional to $1-\theta$

$[A]$ is proportional to the pressure gas, P

Thus another equilibrium constant (b), as $b = \frac{\theta}{(1-\theta) \cdot P}$, θ represents the fraction of surface sites occupied which is in the range of 0-1, and rearrangement gives an expression for the surface coverage:

$$\theta = \frac{bP}{1+bP}$$

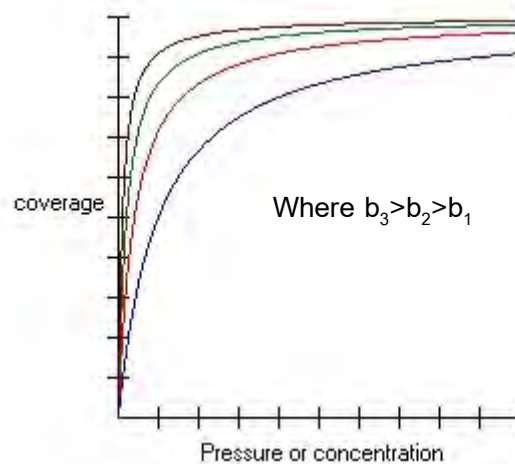


Figure 2.7 The characteristic of graphical form of Langmuir isotherm

When the definition of V_m is the monolayer volume, and V_a is the amount of adsorbed gas at an arbitrary pressure, the equation of the Langmuir plot is

$$\frac{P}{V_a} = \frac{1}{bV_m} + \frac{P}{V_m}$$

Where $V_a = V_m \theta$ and $V_a = \frac{V_m bP}{1+bP}$

The Langmuir plot between $\frac{P}{V_a}$ in y-axis and P in x-axis provides a linear line with $\frac{1}{V_m}$ as slope and $\frac{1}{bV_m}$ as y-intercept.

In addition, for kinetics, the rate of adsorption is proportional to the pressure of the gas and the number of vacant sites for adsorption. The equation of adsorption is given below

$$\frac{d\theta}{dt} = k_a p N (1 - \theta)$$

$$\frac{d\theta}{dt} = -k_d N \theta$$

Where k_a and k_d are the rate constants for adsorption and desorption, respectively, and N is the total number sites on the surface, and p is the pressure of the adsorbate gas. At equilibrium, the coverage is independent of time and the adsorption and desorption rates are equal.

2.3.3.2 Brunauer-Emmett-Teller (BET) adsorption isotherm

In 1938, Stephan Brunauer, Paul Hugh Emmett, and Edward Teller firstly published BET theory in a journal. BET theory is created to explain the characteristic of physical of gas molecules on a solid surface area, and it becomes the important technique for the measurement of specific surface area. Their concept of this is extension of Langmuir theory which describes the nature of adsorption of adsorbate is monolayer and it can adsorb at low pressure with high thermal energy and high velocity. On the other hand, under high pressure and low pressure, the thermal energy of gaseous molecules will decrease and more gaseous molecules is accessible on surface area and can adsorb with multilayer formation. This can explain with the BET equation is followed as

$$\frac{p}{V(p^0 - p)} = \frac{1}{V_m C} + \frac{(C-1)}{V_m C} \cdot \frac{p}{p^0}$$

where V is the amount of N_2 adsorbed at the relative pressure p/p^0 , p and p^0 are the equilibrium and the saturation pressure of adsorbates and V_m is the the monolayer adsorbed gas quantity such as in volume units and C is the BET constant which is expressed as

$$c = \exp\left(\frac{E_1 - E_L}{RT}\right)$$

Where E_1 is the heat of adsorption for the first layer, E_L is the heat of adsorption for the subsequent and higher areas. This heat is equal to the heat of liquefaction.

From BET equation, it can be plotted with $\frac{P}{V(p^0 - p)}$ on the y-axis and $\frac{P}{p^0}$ on the x-axis to form as the straight line. The plot is called BET-plot whose slope and y-intercept of of $\frac{C-1}{V_m \cdot C}$ and $\frac{1}{V_m \cdot C}$, respectively. In the range of $0.05 < \frac{P}{p^0} < 0.35$, the slope and y-intercept value are used for calculation the quantity of monolayer adsorbed gas (V_m) which is the reciprocal of summation of slope and y-intercept following as

$$V_m = \frac{1}{\left(\frac{C-1}{V_m C}\right) + \frac{1}{V_m C}}$$

and BET constant (C) is calculated from the equation below

$$C = 1 + \frac{\left(\frac{C-1}{V_m C}\right)}{\left(\frac{1}{V_m C}\right)}$$

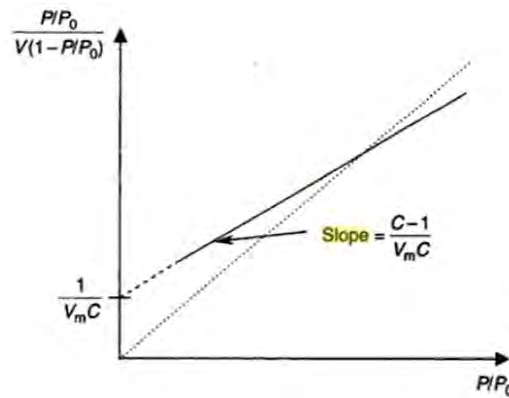


Figure 2.8 BET-plot of any sample [84]

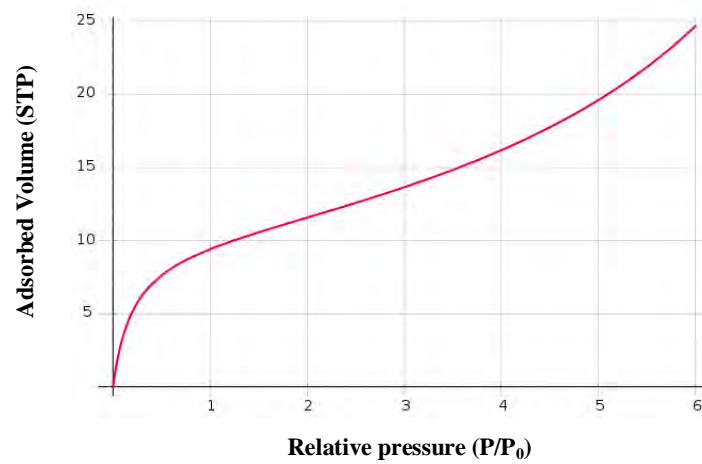


Figure 2.9 An example of BET isotherm

For calculation of a total surface area (A_s) and a specific surface area (a_s), they are calculated with the equation

$$A_s(BET) = V_m \cdot L \cdot a_m$$

$$a_s(BET) = \frac{A_s(BET)}{m}$$

where A_s (BET) and a_s (BET) are the total and specific surface areas, respectively, of the adsorbent, a_m is the average molecular cross-sectional area, L is the Avogadro constant, and m is the mass of adsorbent.

2.3.3.3 Freundlich and Küster isotherm

This curve involves the relation of the concentration of a solute on the adsorbent or in the liquid which is in contact. This isotherm was the first isotherm using mathematical for fitting. It was published by Freundlich and Küster in 1894 and was an empirical formula of calculation of gaseous adsorbates. The Freundlich adsorption isotherm is mathematically expressed as

$$\frac{x}{m} = kP^{\frac{1}{n}}$$

or

$$\frac{x}{m} = kC^{\frac{1}{n}}$$

where x is the quantity of adsorbate, m is the mass of the adsorbent, k and n are the empirical constants at ambient temperature for adsorbent-adsorbate and P is the pressure. When the quantity of adsorbed molecules slowly increases with rising pressure and then higher pressures will increase to saturate the surface, the k and n constant change which influences the empirical observation.

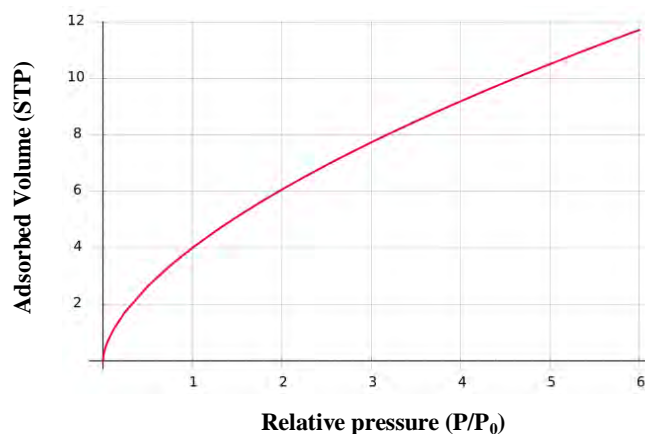


Figure 2.10 An example of Freundlich sorption isotherm

CHAPTER III

EXPERIMENTAL

3.1 Materials

3.1.1 Preparation of silica fibers by electrospinning process

- 1) Tetraethylorthosilicate, 98% (Sigma Aldrich, Germany)
- 2) Absolute ethanol (Merck, Germany)
- 3) Concentrated hydrochloric acid, 36.5-38% (J.T.Baker, Thailand)
- 4) Deionized water

3.1.2 Functionalization of electrospun fibrous silica mats

- 1) Toluene (Merck, Germany)
- 2) 3-(triethoxysilyl)propylamine (Merck, Germany)

3.1.3 Adsorption and elution of formaldehyde in water

- 1) Concentrated formaldehyde solution, 37% (Merck, Germany)
- 2) Concentrated hydrochloric acid, 36.5-38% (J.T.Baker, Thailand)
- 3) Concentrated sulfuric acid, 98% (J.T.Baker, Thailand)

3.1.4 Standardization of formaldehyde solution

- 1) Sodium carbonate anhydrous powder (J.T.BaKer, USA)
- 2) Iodine resublimed (CARLO ERBA, France)
- 3) Sodium thiosulphate (Ajax Finechem, Australia)
- 4) Potassium iodate (Ajax Finechem, Australia)

- 5) Concentrated hydrochloric acid, 36.5-38% (J.T.Baker, Thailand)
- 6) Concentrated sulfuric acid, 98% (J.T.Baker, Thailand)
- 7) Sodium hydroxide (CARLO ERBA, France)
- 8) Starch solution, 1%
- 9) Concentrated formaldehyde solution, 37% (Merck, Germany)

3.1.5 Determination of formaldehyde by spectrophotometric method

- 1) 2,4-Pentane dione (Acetyl acetone) (CARLO ERBA, France)
- 2) Ammonium acetate (Scharlau, Spain)
- 3) Glacial acetic acid (Merck, Germany)

3.2 Methodology

3.2.1 Preparation of silica fibers

The preparation of silica sol used for electrospinning process was followed by Choi, Sung-Seen and coworkers [19]. Firstly, silica sol was synthesized by using tetraethyl-orthosilicate (TEOS), ethanol (EtOH), deionized water and concentrated hydrochloric acid (HCl) with the molar ratio of 1:2:2:0.01, respectively. The 23 mL of the mixture of TEOS and EtOH was continuously stirred and dropped by 50 μ L concentrated hydrochloric acid and 2.4 mL deionized water. The solution was heated at 70-80°C about 30-60 minutes. The liquid sol becomes clearly viscous sol because of solvent evaporation and polymerization. Later, the viscous silica sol was transferred into 5-mL disposable syringe with hypodermic needle of 0.80 mm diameter. This syringe was fixed on a syringe pump (NE-1000, Prosense) which was set a flow rate at 20 μ L/min. A high voltage power supply (230 series, Bertan High Voltage Research) was used for charging the sol between syringe needle and

collection screen. This needle was connected to the power supply with positive output. The electric potentials of 10, 15 and 20 kV were studied. In the part of collection screen, it was copper plate covered with aluminium foil and perpendicularly attached to the syringe needle with the various distances of 5, 10 and 15 cm. Amount of 500 μL sol was approximately used for a fibrous silica mat on the plate for 25-30 minutes. After that, the obtained eletrospun fibrous silica mats were dried in an oven at 80-100°C for solvent evaporation.

3.2.2 Preparation of the functionalized fibrous silica mats with 3-aminopropyltriethoxysilane (APTES)

Before modification, some electrospun fibrous silica mats were dried in an oven at 100-150°C for 3 hours in order to remove moisture. Afterward, the fibrous silica sheets were returned to room temperature. One hundred milligram of these sheets was weighed on an analytical balance (Mettler AT200) and put into a rounded bottom flask. The fibrous silica mats were subsequently immersed in 30 mL of the mixture of APTES in dried toluene at various concentrations of APTES including 0.10, 0.15, 0.25, 0.5, 0.75, and 1.00 M. Next, this portion was refluxed under nitrogen gas at 70-80°C for 24 hours. The obtained functionalized silica fibers mats were filtered and washed with dried toluene 2-3 times. Lastly, these mats were dried overnight at 80°C in an oven for removal of solvent and moisture.

3.2.3 Characterization of functionalized electrospun silica fibers

3.2.3.1 Fourier-Transform Infrared Spectrometry (FT-IR)

Functional groups of functionalized and non-functionalized electrospun fibrous silica mats were identified with FT-IR (Impact 410: Nicolet) by KBr pellet with a range of 40-4000 cm^{-1} wavenumber and 4 scans with resolution of wavenumber of $\pm 4 \text{ cm}^{-1}$ in mode of transmittance.

3.2.3.2 Scanning Electron Microscopy (SEM)

The morphology of electrospun fibrous silica mats were characterized by a JEOL Scanning Electron Microscope (model JSM-5410 LV). Silica fibers samples were adhered to a stub with carbon tape and coated with gold in order to minimize charging effect. SEM images with magnifications of 1500x and 7500x were used for morphology and size characterization. Image Tool 3.0 software (Shareware provided by UTHSCSA) was used for estimation of diameters of these silica fibers mats. Fifty different fibers in image were randomly chosen and measured.

3.2.3.3 Thermogravimetric Analysis (TGA)

Aminopropyl groups on functionalized silica fibers were examined and compared with non-functionalized one by Thermogravimetric analyzer providing measurement of a weight loss of material associated with transition and thermal degradation. Sample weight for analysis was about 2-3 grams. Before this study, silica fibers mats were grinded to powder for heating in the range of 50-900°C at heating rate of 25-30°C/min. TGA thermogram showed the loss of aminopropyl functionalized group on silica sample as the percentages compared with the initial weight of sample.

3.2.3.4 Surface area analysis

The nitrogen adsorption isotherms of modified silica fibers with various APTES contents including 0.00, 0.15, 0.50, and 1.00 M were measured. Prior to adsorption measurement, the different concentrations of fibrous silica mats (about 30-40 mg) were placed in the tubes and pretreated under vacuum at 300°C for 2-3 hours and subsequently absorbed with a surface area analyzer (BELSORP mini). The Brunauer-Emmett-Teller (BET) equation from adsorption isotherms were calculated for determination of surface area, and total pore volume. Pore size distribution was investigated with Barrett-Joyner-Halenda (BJH) theory for

explanation the characteristic of adsorption on the surface area of silica fibers. For total pore volumes, they were determined from adsorbed nitrogen at P/P_0 value 0.990.

3.2.3.5 Elemental analysis (EA)

Carbon, nitrogen, and hydrogen content in the functionalized silica mats were characterized with the CHNS Leco-932 Elemental analyzer. Six quantities in the range of 1.900-2.000 mg of sulfa-methazine were used for standard calibration. The samples for test were weighed in tin capsules with required amounts of 1.950-2.100 mg. After folding these capsules, the samples were placed in the autosampler for combustion. Quantitative analysis of these element were repeated three times for one sample and the results were shown in the percentage of carbon (C), nitrogen (N), hydrogen (H) and sulfur (S).

3.2.4 Study of efficiency of functionalized silica fiber

3.2.4.1 Adsorption of formaldehyde solution

One thousand part per million (ppm) of formaldehyde stock solution was prepared from concentrated formaldehyde solution (37%) and standardized before use. Ten ppm formaldehyde solution was diluted from the stock solution and used as a working standard solution.

The $1 \times 1 \text{ cm}^2$ of APTES functionalized and non-functionalized fibrous silica mats were weighed about 3-4 mg and were immersed into 10 ppm formaldehyde solution in the closed glass vial at room temperature. Results of times such as 1, 3, 6, 12, 18 and 24 hours and different concentrations of aminopropyl functionalized fibrous silica mats including 0.10, 0.15, 0.25, 0.50, 0.75, and 1.00 M for adsorption of formaldehyde solution were studied.

3.2.4.2 Elution of formaldehyde solution

Elution study was evaluated with the optimum adsorption condition. The adsorbed formaldehyde silica mats were immersed in different types of acid solution: hydrochloric acid and sulfuric acid with manifold concentrations: 0.1, 0.5, 1.0, 1.5, 2.0, and 3.0 M. Various times for formaldehyde elution which were 15, 30, and 60 minutes were examined.

CHAPTER IV

RESULTS AND DISCUSSION

This chapter is divided into four sections. Firstly, the morphology of silica fibers prepared by electrospinning process and the functionalized silica fibers with APTES were evaluated. Secondly, the characterizations of non-functionalized and functionalized electrospun silica fibers were shown. Then, the efficiency of functionalized electrospun silica fibers in adsorption of formaldehyde in water was studied. Finally, the elution of adsorbed formaldehyde from functionalized electrospun silica fibers with acids was examined.

4.1 Morphology of electrospun fibrous silica mats

The silica sol prepared by mixing of tetraethylorthosilicate (TEOS), ethanol (EtOH), deionized water, and concentrated hydrochloric acid (HCl) in molar ratio of 1:2:2:0.01 was applied for electrospinning process. Silica sol was stretched and formed to cone shape by high electric field. Reaching to the critical voltage, the stretching flight jet of viscous sol was spouted to the aluminum foil on a copper plate collection screen with electric force: positive charge on sol and negative charge at this collector, and then the white non-woven nanofibrous silica mats would appear on this collection screen. Different shapes of the resultant electrospun fibrous silica mats depended on the electric potential and distances between syringe needle and collection screen.

4.1.1 Electrospun fibrous silica mats before functionalization

Because electric field and distance between syringe needle and collector were concurrently affected the characteristic of fibrous mat, they were simultaneously selected for optimum condition.

The SEM images of electrospun fibrous silica mats at various distances (5, 10, and 15 cm) and electric potentials (10, 15, and 20kV) were shown in Figure 4.1. Most of electrospun silica fibers were uniform, smooth, straight and no linkage. Beads formations were clearly observed when electrospinning at the distance of 5 cm and the electric field of 10 and 15 kV. The fibers derived at low electric field (10 kV) were also irregular and unequal sizes, although their appearances were in fibrous form. Average diameters of silica fibers (n=50) were in the range of 200-270 nm which were summarized in Table 4.1.

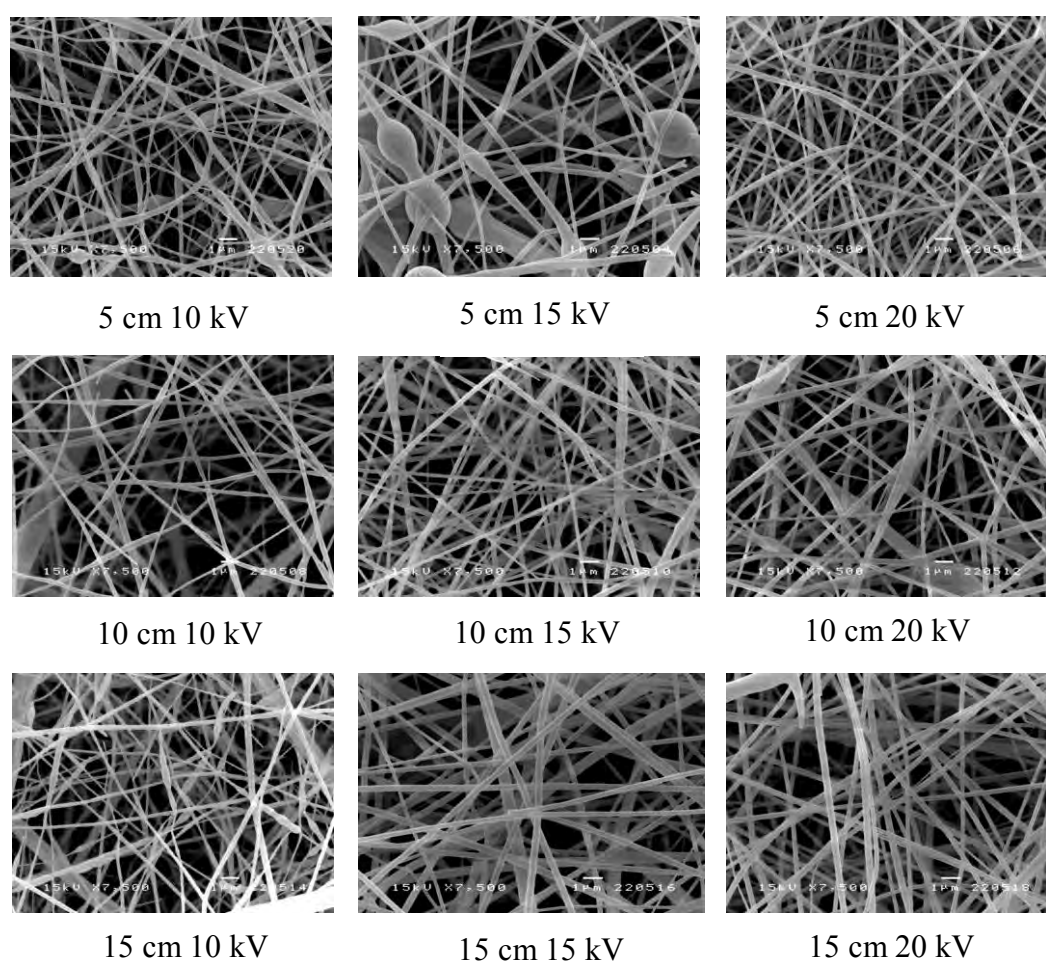


Figure 4.1 SEM images of electrospun silica fibers obtained from 9 conditions by changing the electric fields and distance between syringe needle and collection screen. Original magnifications 7,500x.

At fixed distances, an increasing of electric field affected the size of silica fibers. Their diameters should be smaller than one which was electrospun at lower electric field due to more stretching of fibers. When considering the average diameters of electrospun silica fibers at conditions of fixed distance of 5 cm and various electric fields of 10, 15, and 20 kV in Table 4.1, the diameter of these fibers would decrease from 228 nm to 214 and 211 nm, respectively. This result was in accords with the mention above. On the contrary, electrospun silica fibers achieved from longer distance (10 and 15 cm), spinning at high electric fields had the larger average diameters, which were different from the previous mention. This can be the result of low stretching and a simultaneously rapid spouting of jet flowed toward the collector.

Table 4.1 Fiber formation and average diameter of fibers

Distances (cm)	Electric potential (kV)	Fiber formation	Average diameter of fibers (nm) (n=50)
5	10	Bead fibers	228±75
	15	Bead fibers	214±82
	20	Bead fibers	211±62
10	10	Fibers	230±88
	15	Fibers	226±86
	20	Fibers	268±102
15	10	Fibers	201±96
	15	Fibers	259±75
	20	Fibers	257±89

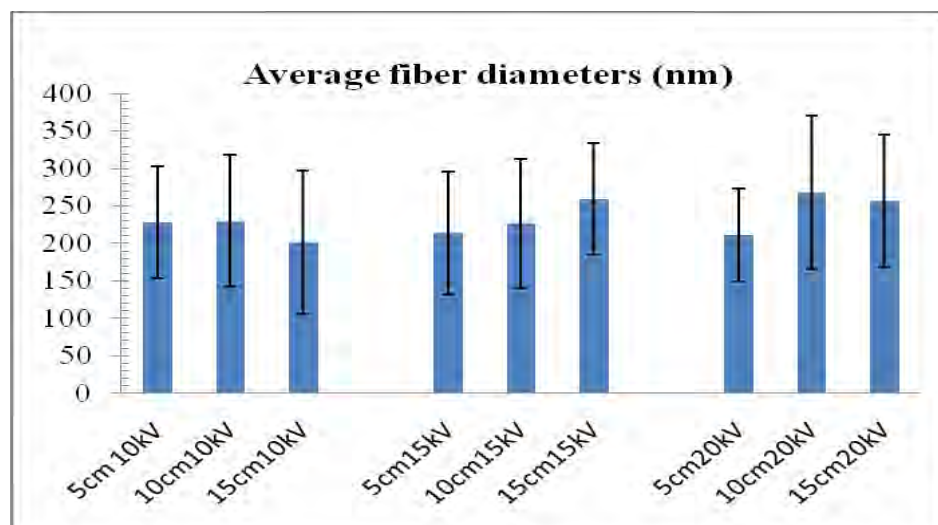


Figure 4.2 Average diameters of electrospun fibers at various electric potentials and distances between the needle and the collection screen

The fibers from electrospinning at condition of 5 cm with 10 kV and 15 kV had bead formation because of using high voltage and too short distance. Therefore, irregularity of stretched fibers and rapid evaporation of solvent were simultaneously occurred. As the electric field was increasingly used for fibers production, the size of beads should also be diminutive. This observation was able to consider from bead size derived at distance of 5 cm and electric field of 15 kV and 20 kV.

Characteristic of silica fibers at 10 cm, 15 cm and low electric field of 10 kV from SEM images were irregular and not smooth. In virtue of spinning at far distance with low electric field, a spouting of flight jet toward the collector were discontinuously produced and a little beads were formed. Additionally, sol jet would slightly stretch and partially spout to the collector but most of them were on the ground between the needle and the collection screen. The appearances of resulting fibers were thinner than other conditions because there is only enough strong stretching jet which could be electrospun to the collection. Moreover, it needed to take a long time in electrospinning process to obtain enough fibers for applications. Subsequently, these conditions: the distance of 10 cm and 15 cm at electric field of 10 kV was not chosen for optimum condition for electrospinning.

For conditions of 10 cm 20 kV, 15 cm 15 kV, and 15 cm 20 kV, the average diameters of obtained fibers were in the range of 260-270 nm, which were bigger than one of other conditions. This can describe with the result from high electric potential, the acceleration of silica sol jet to collection screen with short time were taken place that corresponds to the inconsistent stretching of jet. In point of capacity of silica, efficiency of adsorption with these big silica fibers was less than smaller ones because of lower surface areas to volume ratio. Furthermore, silica sol jet would be widespread out all instruments set up at high electric field and long distance; therefore, amount of silica fibers for real application were diminished. Summarily, these mentioned conditions were not chosen for adsorption.

In conclusion, electric potential and distance between needle and collection screen had not significantly affect the size of electrospun silica fibers. Although silica fibers derived from spinning with distance of 5 cm and high electric potentials of 10, 15, and 20 kV were small, the bead formations on fibers were appeared. Moreover, the high dense silica fibers were on only central collector that this result affects to the reduction of surface area for adsorption efficiency. In addition, the electric sparks could easily be observed due to shot jet with short distance and high electric potential. The optimum condition for electrospinning was distance between the needle and the collector of 10 cm and electric potential of 15 kV.

4.1.2 Electrospun silica fibers after functionalization with 3-aminopropyltriethoxysilane (APTES)

After functionalization with 3-aminopropyltriethoxysilane (APTES), the morphology of electrospun fibrous silica mats were changed. In Figure 4.3, the SEM images of electrospun fibrous silica mats functionalized with various concentrations including 0.10 M, 0.15 M, 0.25 M, 0.50 M, 0.75 M and 1.00 M APTES were shown.

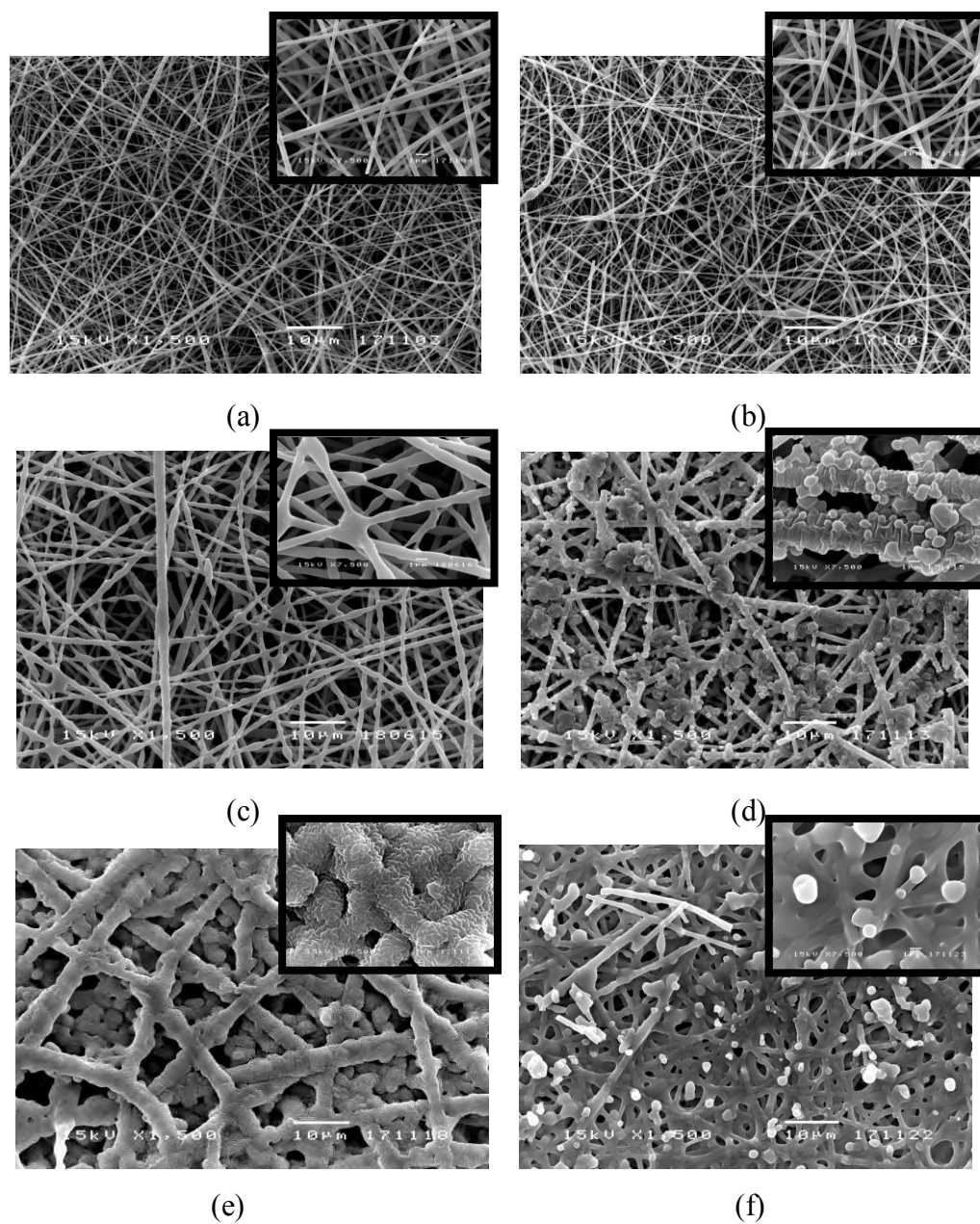


Figure 4.3 SEM images of electrospun silica fibers mats functionalized with (a) 0.10 M (b) 0.15 M, (c) 0.25 M, (d) 0.50 M, (e) 0.75 M, and (f) 1.00 M APTES. Original magnifications 1,500 x (big images) and 7500 x (small images).

The shapes of functionalization silica fibers mats were different depending on the concentration of APTES. If high quantities of APTES were used in functionalization of electrospun silica fibers, the appearances of these fibers would be gnarled, irregular, nodes on the main fibers and many linkages like a lump which resulted from self-polymerization of excess APTES molecules. APTES

concentrations for functionalization were directly concerned because fiber sizes were increased and many bulks on these fibers achieved from self-polymerization. In general, APTES can graft on silica fibers by reacting to siloxane bond in structure of silica and also self-react with APTES molecules.

Normally, the silane coupling agent, 3-aminopropyltriethoxysilane (APTES) has three bonds of EtO-Si and one bond of aminopropyl group (-C₃H₆NH₂).

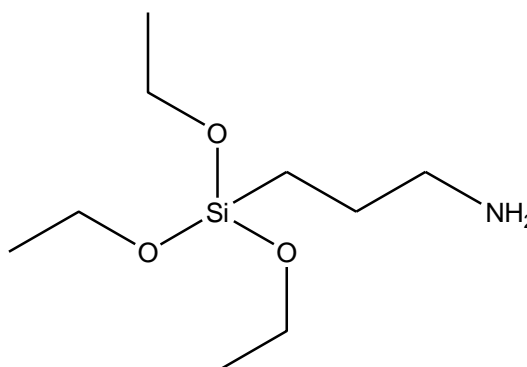
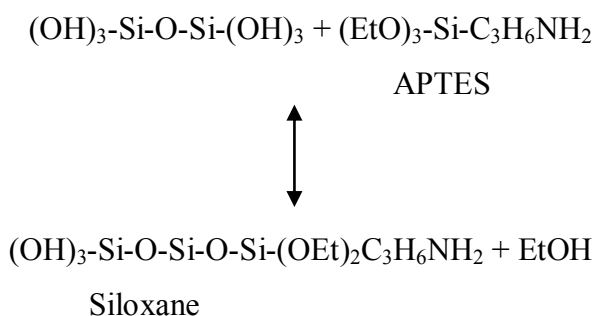


Figure 4.4 The structure of 3-aminopropyltriethoxysilane (APTES)

In this regard, three EtO-Si bonds in APTES structure can react with free silanol groups (-Si-OH) on the surface of electrospun fibrous silica mat and transform into Si-O-Si bonds via condensation called the grafting process resulting of aminopropyl group on silica in Scheme 4.1. Moreover, APTES molecules can also polymerize together instead of grafting as in Scheme 4.2.



Scheme 4.1 Grafting process of aminopropyl group on silica



Scheme 4.2 Self-polymerization of APTES

Average diameters of modified silica fibers of all concentrations were summarized in Table 4.2. The size of silica fibers at the least concentration of APTES (0.10 M) was bigger than one of non-functionalization fibrous silica mats about 1-2 folds, but smaller than functionalized silica fibers with other concentrations of APTES. For 1.00 M APTES, appearance of fibers was not in fiber form and difficult to count the number of fibers; therefore, the fiber diameters of this condition were not measured.

Table 4.2 Average diameter of fibers functionalized with various APTES concentrations

Concentration of APTES for modification	Average diameter of fibers (nm) (n=50)
0 M	226±86
0.10 M	330±120
0.15 M	360±160
0.25 M	1300±200
0.50 M	1650±400
0.75 M	3520±620
1.00 M	Not in fiber form

With considering both the images and the average diameters of fibers at all conditions, it could mention that the functionalized silica fibers could be synthesized in the range of APTES contents between 0.10-0.75 M. If they were grafted this coupling agent with concentration more than 0.75 M, the fiber form of silica were decreased and become a bulk.

The size of silica fibers affected the efficiency of adsorption of formaldehyde. With various concentrations of APTES, the size of modified silica

fibers was different. Addition to the size, surface area, pore diameter, and amino group content of modified silica fibers would relate to the adsorption efficiency of formaldehyde. With this advantage, these fibrous silica mats can be widely used in many applications. However, the efficiency of functionalized fibrous silica mats for formaldehyde adsorption from only results of SEM images was not enough for conclusions. Other techniques such as FT-IR, TGA, elemental analyzer and surface area analyzer were necessarily used for additional supports and helping for implication in the efficiency of formaldehyde adsorption.

4.2 Characterization of non-functionalized and functionalized electrospun fibrous silica mat with APTES

4.2.1 Fourier-transform Infrared Spectrophotometry (FT-IR)

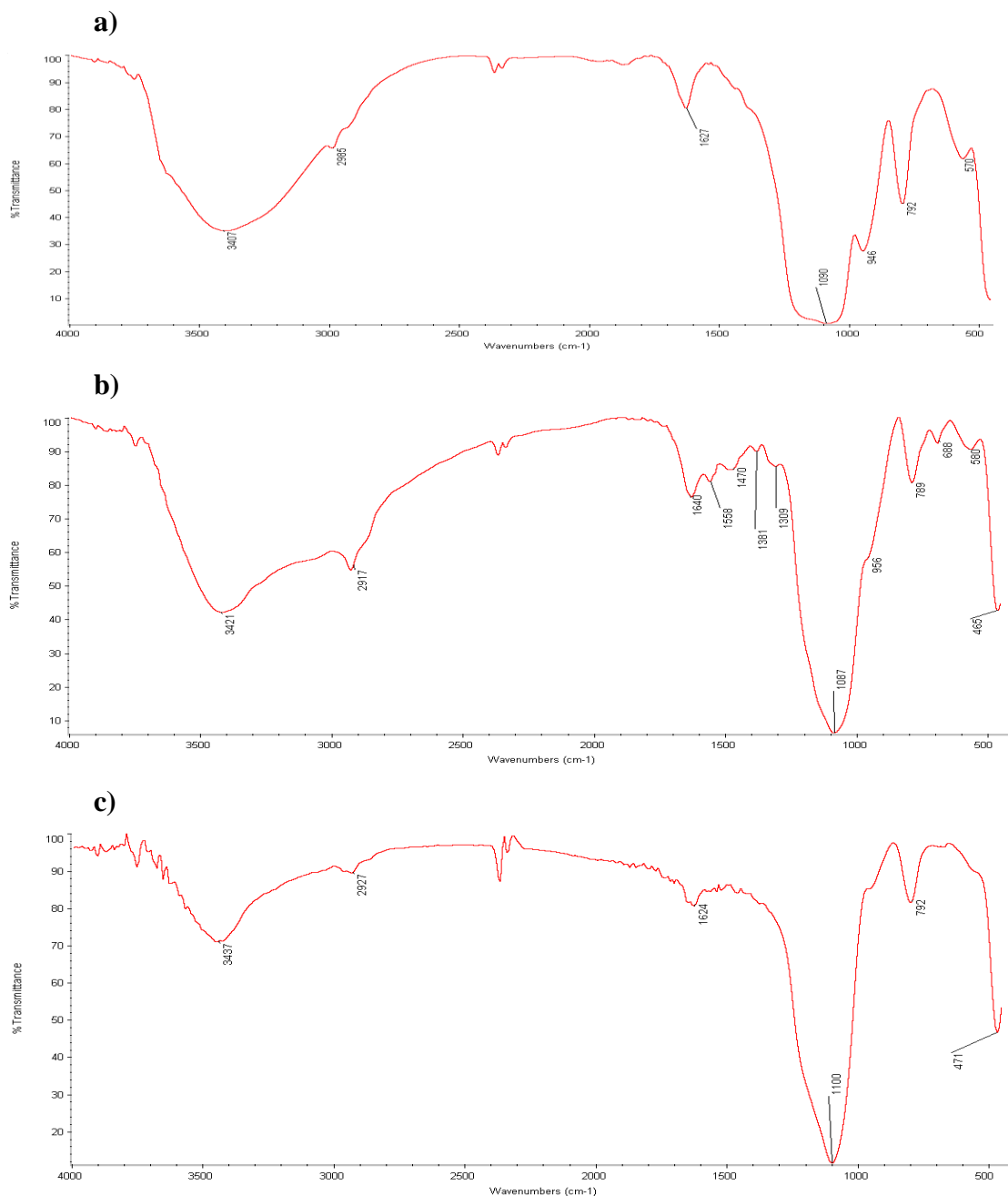


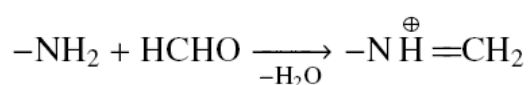
Figure 4.5 The IR spectrum of electrospun fibrous silica mats of (a) non-functionalization, (b) aminopropyl functionalization with APTES and (c) aminopropyl functionalization after formaldehyde adsorption

The fibrous silica mats of non-functionalization and functionalization with APTES were characterized with FT-IR. The characteristics peaks of non-functionalized and functionalized fibrous silica mats before and after formaldehyde adsorption were summarized in Table 4.3. The strong and broad band at 3000-3600 cm^{-1} (especially, 3407 cm^{-1}) and a sharp peak at 1627 cm^{-1} of silica fibers in Figure 4.5 (a) indicated the presence of O-H bond (hydrogen bonding) in silanol group (Si-OH) on silica surface [59]. This group, derived from acid catalyzed hydrolysis of TEOS, changed ethoxy group ($-\text{OC}_2\text{H}_5$) to form silanol group. Meanwhile, a peak at the same position of functionalized silica fibers in Figure 4.5 (b) was sharper due to the additional presence of N-H stretching of amine in aminopropyl group (3421 cm^{-1}). Additionally, a broad band of NH_3^+ stretching at 2800-3400 cm^{-1} coexistingly overlapped the band of O-H stretching from silanol group and the clear appearance of peak of aliphatic C-H stretching of ethyl group in ethoxy group ($-\text{OC}_2\text{H}_5$) remained in silica structure and propyl group ($-\text{C}_3\text{H}_6$) in aminopropyl group ($-\text{C}_3\text{H}_6\text{NH}_2$) of functionalized silica at 2900-3000 cm^{-1} were shown. With observation in both of Figures 4.5 (a) and (b), apart from the sharper peak at 2800-3400 cm^{-1} , there was a difference between the bands of both IR spectrum at around 1400-1600 cm^{-1} which were assigned to the symmetric bending vibration of $-\text{NH}_2$ at 1558 and 1470 cm^{-1} [59] of functionalized silica fiber. The peak assigned for Si-CH₂ stretching bands around 1150 cm^{-1} could not clearly identified because it may overlap with the strong peak attributed to vibration of Si-O-Si band at 1090 cm^{-1} . Besides, there was also other bands such as 956, 789, 580, 465 cm^{-1} which corresponded to symmetric and asymmetric vibration bands [59]. Regarding to this observation, aminopropyl group can be successfully grafted on electrospun silica fibers to obtain functionalized silica fibers.

Table 4.3 The IR characteristic peaks of non-functionalized silica fibers (-SiO₂), functionalized silica fibers with APTES (-SiC₃H₆NH₂) and functionalized silica fibers with APTES after formaldehyde adsorption (-Si-C₃H₆N=CH₂)

Wavenumber (cm ⁻¹)	Functional group of		
	-SiO ₂	-SiC ₃ H ₆ NH ₂	-Si-C ₃ H ₆ N=CH ₂
3000-3650	O-H stretching of silanol group	O-H stretching of silanol group, N-H stretching of amine	O-H stretching of silanol group
2850-2970	C-H stretching of aminopropyl group	C-H stretching of aminopropyl group	C-H stretching of aminopropyl group
1600-1640	O-H bending of silanol group	O-H bending of silanol group	-
1640-1690	-	-	-C=N- stretching of imine
1400-1650	-	N-H bending of amine	N-H bending of amine
1025-1200	-	C-N stretching of aminopropyl group	C-N stretching of aminopropyl group
700-1000	Si-O-Si vibration of siloxane	Si-O-Si vibration of siloxane	Si-O-Si vibration of siloxane

The IR characteristics peaks of the functionalized silica fibers after formaldehyde adsorption in Table 4.3 resembles the IR peaks of the functionalized silica fibers before adsorption, exception the peak at 1640-1690 cm⁻¹ which is more prominent than that because there is a presence of imine (-C=N-) band which is the product of reaction between formaldehyde and amine in functionalized fibers [15] as



Scheme 4.3 Imine formation

This indicated that there is the occurrence of the adsorption of formaldehyde and imine formation on the silica surface.

4.2.2 Elemental analysis (EA)

The percentage of elements in samples, particularly carbon (C), hydrogen (H), and nitrogen (N) were measured to quantify the aminosilane grafted on fibrous silica surface. From raw data, the percentage of carbon, hydrogen, and nitrogen in each samples were shown in Table 4.4.

Table 4.4 The percentage of average amount of some elements from elemental analyzer

Silica fiber mat functionalized with	Average amount of elements analyzed (%) (n=3)			Carbon (C):Nitrogen (N) ratio
	Carbon (C)	Hydrogen (H)	Nitrogen (N)	
0 M APTES	0.481±0.040	1.424±0.016	0.053±0.004	-
0.15 M APTES	13.360±0.054	4.175±0.020	4.731±0.011	2.824
0.5 M APTES	17.840±0.331	4.997±0.007	6.192±0.047	2.881
1.0 M APTES	19.373±0.265	4.939±0.019	7.043±0.044	2.752

In consideration of the result in Table 4.4, the percentages of carbon and nitrogen gradually increase with the addition of APTES concentration while the C:N ratio was constant. From calculation based on the molecular weight of functional group (-C₃H₆NH₂), the ratio of carbon and nitrogen was 2.57 which defined as theoretical value. The results of C:N ratio in functionalized fibrous silica mat at all APTES addition closed to this value, but they were higher than theoretical value. This can be explained that quantities of carbon were not only in the form of functional group (-C₃H₆NH₂) but also were in ethoxy group (-OC₂H₅) remaining in the structure due to incompleteness of polymerization reaction between silanol groups. The results

also proved the additional functional group of aminopropyl ($-C_3H_6NH_2$), when APTES was increased, the amount of carbon and nitrogen reasonably extended.

4.2.3 Thermogravimetric analysis (TGA)

The characterizations of electrospun fibrous silica mats by Thermogravimetric Analyzer (TGA) were examined to determine the quantities of aminopropyl group on silica fibers. The APTES concentrations of 0 (non-functionalization), 0.10, 0.50, and 1.00 M, were studied as shown in Figure 4.6. For TGA curves of functionalized fibrous silica mats (Figure 4.6 b-d), two steps of weight loss were observed which corresponding to the loss of adsorbed moisture, trapped residual ethanol on silica surface and probable decomposition of unreacted APTES in early heating before 200°C and the second stage was the loss of aminopropyl functional group in range of 400-600°C [85].

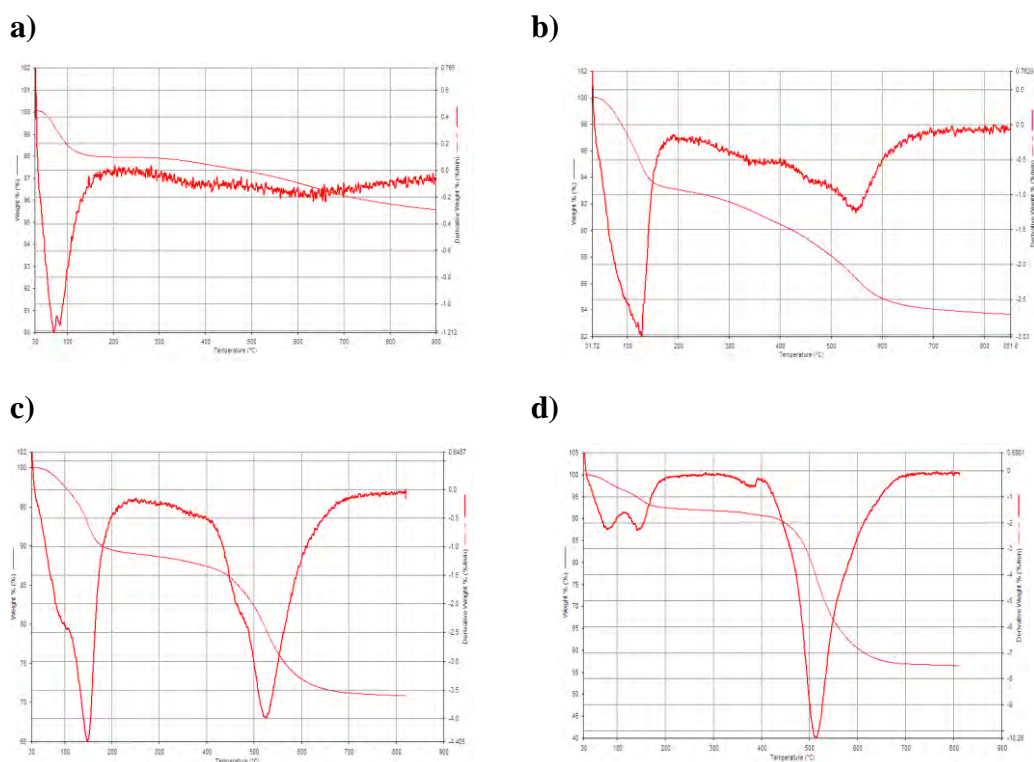


Figure 4.6 Thermogravimetric analysis (TGA) curves of electrospun silica fibers mat with: (a) non-functionalization, and functionalization with (b) 0.10 M (c) 0.50 M (d) 1.00 M 3-aminopropyltriethoxysilane (APTES)

From Figure 4.6, when APTES content of modified silica increases, a loss of this functional group would as well increase by consideration of the height of a second step in TGA curve or the second peak height in DTA curve (in the temperature between 400-600°C). Therefore, a loss aminopropyl group directly related to APTES functionalized concentrations. Besides, the result of the comparison of characteristic of non-functionalized silica and functionalized silica curves detailed that the unmodified silica curve did not show any change weight after heating above 200°C which was different from curve of modified silica. It can conclude that the aminopropyl group could be successfully modified on silica surface and the loss quantities of aminopropyl group were varied with amount of APTES for functionalization. The percentages of a loss of aminopropyl group were used to calculate grafting percentage and loading capacity of this functional group from three functionalized conditions in Table 4.5.

Table 4.5 Grafting percentage and loading capacity of aminopropyl group into electrospun fibrous silica mats

APTES concentration (mol/dm ³)	APTES concentration in dry toluene (theoretical loading capacity) (mmol/g)	% loss of aminopropyl group	% grafting	loading capacity (mmol/g)
0.10	7.9	8.87	10.76	1.56
0.50	39.6	17.78	25.79	3.14
1.00	79.3	34.45	61.88	6.07

The percentage of a loss aminopropyl group, % grafting and loading capacity directly related to APTES concentrations. The percentage of grafting could be calculated from quotient of amount of aminopropyl group and weight of silica sheet, which did not include weight of adsorbed moisture and functionalized aminopropyl group, multiplied with 100 as the equation below:

$$\% \text{ Grafting} = \frac{\text{a loss weight of aminopropyl group } (-\text{C}_3\text{H}_6\text{NH}_2) \text{ (g)}}{\text{silica sheet (g)}} \times 100$$

Loading capacity values obtained from three functionalized conditions shown in Table 4.6 were calculated from this equation:

$$\text{Loading capacity} = \frac{\text{aminopropyl group } (-\text{C}_3\text{H}_6\text{NH}_2) \text{ (g)}}{\text{M.W. of } (-\text{C}_3\text{H}_6\text{NH}_2) \times \text{silica fibers (g)}}$$

A unit of loading capacity was mole or millimole per gram. This value indicated the amount of loading of aminopropyl group onto fibrous silica mat surface. In comparison between APTES concentration in dry toluene and loading capacity, the quantities of APTES in toluene was higher than APTES grafted amount. This result was in accord with the research of Mathieu Etienne, Alain Walcarius [86] which reported that the quantity of grafted aminosilane was always less than the initial quantity of APTES in the synthesis medium, indicating the occurrence of an equilibrium between physically adsorbed and non-adsorbed APTES molecules on silica in toluene.

From Table 4.5, the percentages of grafting, and loading capacity had increase when APTES concentrations were increasingly used. With these results, silica fibers could be functionalized with aminopropyl group on their surface successfully and % grafting and loading capacity were varied with amount of APTES for functionalization.

With the consideration of the concordant results from TGA and elemental analysis, it can guarantee the additional of aminopropyl functional group which % grafting were increased as the increment of APTES applied.

4.2.4 Surface area analysis

The nitrogen adsorption isotherms for modified silica fibers with various APTES contents including 0, 0.15, 0.50, 1.00 M were shown in Figure 4.7. The surface area, average pore diameters, and total pore volumes of these samples were

calculated with Brunauer-Emmett-Teller (BET) method and pore size distribution was examined by Barrett-Joyner-Halenda (BJH) theory.

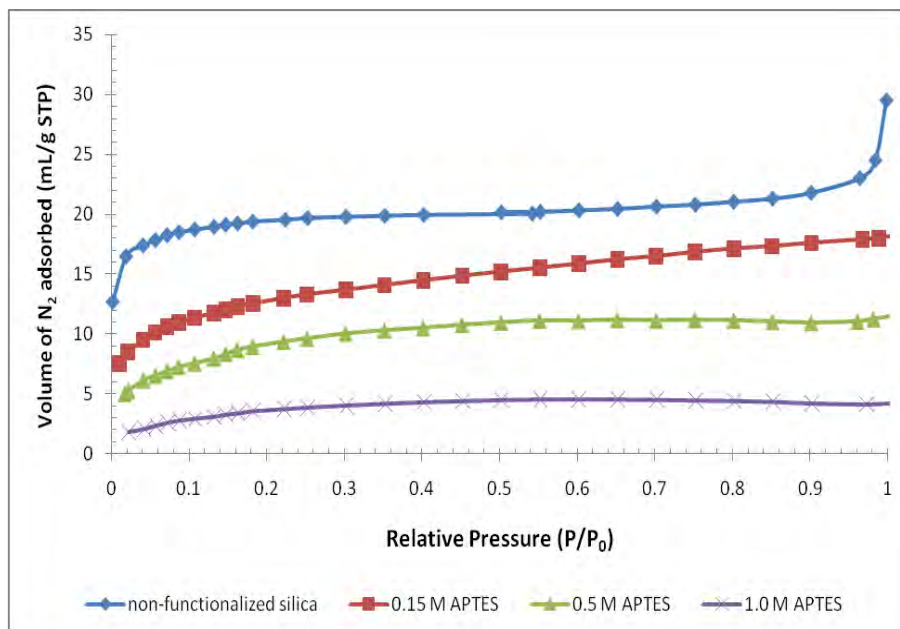


Figure 4.7 Nitrogen adsorption isotherms of non-functionalized fibrous silica mat, and fibrous silica mats functionalized with 0.15M, 0.5M, and 1.0M APTES, respectively.

According to Figure 4.7, the characteristics of adsorption isotherm showed a type of porous materials. Isotherms of non-functionalization and functionalization with various APTES on silica surface cannot be specified to any type following the IUPAC (International Union of Pure and Applied Chemistry) but they related to type IV of mesoporous material [83]. Additionally, the adsorbents contain a little specific surface area and the pore on their silica fibers surface are mesoporosity which pore size were in the range of 2 and 50 nm. Consequently, it was possible that the adsorbents are classified as type IV isotherm. This isotherm type is presented to monolayer-multilayer adsorption because the same path as the part of Type II isotherm which derived from the adsorption process on the surface of adsorbent in non-porous form which corresponds to monolayer adsorption and a loop is generated by capillary condensation of adsorbate in the mesopores.

According to the mono-multi layer adsorption on the adsorbent surface, BET gas adsorption method can be applied to determine the surface area of fibrous silica mats. With the Brunauer-Emmett-Teller (BET) gas adsorption method, it can be applied to be the BET equation (1) in linear form as

$$\frac{p}{V(p^0 - p)} = \frac{1}{V_m C} + \frac{(C-1)}{V_m C} \cdot \frac{p}{p^0} \dots\dots\dots(1)$$

where V is the amount of N_2 adsorbed at the relative pressure p/p^0 and V_m is the monolayer volume and C is the BET constant and the plot between $\frac{p}{V(p^0 - p)}$ and $\frac{p}{p^0}$ are in the linear relationship with the slope of $\frac{C-1}{V_m \cdot C}$ and $\frac{1}{V_m \cdot C}$ as y-intercept.

BET Plots of non-functionalized and functionalized fibrous silica mats were shown in Figure 4.8. The slope and correlation coefficient were summarized in Table 4.6.

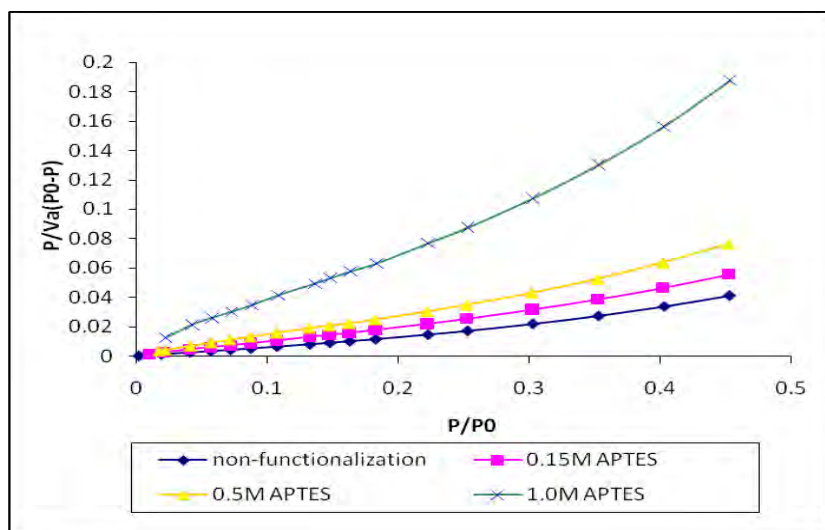


Figure 4.8 BET-Plots of non-functionalized silica fibers, silica fiber functionalized with 0.15 M APTES, 0.50 M APTES, and 1.00 M APTES, respectively.

Table 4.6 Variables from BET-Plots of non-functionalized and functionalized silica fibers

Types of electrospun fibrous silica mats	Slope	Correlation coefficient (r)	Monolayer volume (V_m) [$\text{cm}^3(\text{STP})\text{g}^{-1}$]
Non-functionalization	0.0592	0.9999	16.890
0.15 M APTES	0.0941	0.9999	10.568
0.50 M APTES	0.1259	0.9990	7.802
1.00 M APTES	0.3041	0.9985	3.201

In observation of the experimental data in Table 4.6, the results were found to fit well to BET-Plot in term of correlation coefficients which obviously indicated the linear relationship. Consequently, the results of BET Plot can be used for calculation of specific surface area, pore volume. The slopes of BET-Plots of functionalized fibrous silica mat with three different APTES contents were higher than of non-functionalization and directly associated with increasing in APTES concentrations. The slope of BET plot was inversely related with V_m standing for monolayer volume; therefore, the volume of pore would decrease at high APTES concentration.

From the BET Plots, a surface area can be calculated from monolayer volume and average area which is occupied by adsorbate molecule in the complete monolayer. The equations are expressed as

$$A_s(BET) = V_m \cdot L \cdot a_m \dots\dots\dots (2)$$

$$a_s(BET) = \frac{A_s(BET)}{m} \dots\dots\dots (3)$$

where A_s (BET) and a_s (BET) are the total and specific surface areas, respectively, of the adsorbent, a_m is the average molecular cross-sectional area, L is the Avogadro constant, and m is the mass of adsorbent. The results of BET surface area, total pore volume, and average pore diameter of various APTES contents grafted on electrospun fibrous silica mat were calculated and summarized in Table 4.7.

Table 4.7 Pore characteristics and surface area of electrospun fibrous silica mats

Electrospun fibrous silica mat functionalized with	BET specific surface area, S_{BET} ($\text{m}^2 \text{g}^{-1}$)	Total pore volume, V_p ($\text{cm}^3 \text{g}^{-1}$)	Average pore diameter, D_p (nm)
Non-functionalization	73.512	0.041196	2.2140
0.15 M APTES	45.981	0.027849	2.4226
0.5 M APTES	33.960	0.017552	2.0673
1.0 M APTES	13.932	0.006480	1.8605

From Table 4.7, when APTES content was increased, the specific surface area of the functionalized fibrous silica mats considerably decreases. In addition, both of pore volumes and average diameters of pore were significantly decrease upon increasing APTES concentrations. These factors directly related to specific surface area. When specific surface area decreases, the average diameters and pore volume simultaneously reduce. These results agreeably conform to the SEM images of Figure 4.3. When APTES contents were increasingly used, the production of fiber form was decreased. The fiber size was increase and having many connections, which lead to the bulk form. This indicated that the specific surface area, pore volume, and average pore diameters basically decrease. However, average pore diameter of the fibers from functionalization with 0.15 M APTES has higher than of non-functionalization. It is caused by a simultaneous polymerization and overlapping of silica fibers.

In observation of BET specific surface area in Table 4.7, these values, particular at functionalized with 0.15 M and 0.50 M APTES, was higher than surface area of aminopropyl functionalized rice husk ash reported in the research of Imyim and coworker [87] which was $22.88 \text{ m}^2/\text{g}$. Moreover, the surface area of functionalized fibrous silica mat was not quite different from the surface area of functionalized silica particles with aminopropyl group in the research of Bois and coworkers [88] ($62\text{-}65 \text{ m}^2/\text{g}$). Apart from functionalized silica, BET specific surface area of non-functionalized silica fibers in Table 4.7 ($73.512 \text{ m}^2/\text{g}$) was similar to surface area of mesoporous silica materials of Wang and coworkers [89] which was

75 m²/g and more than the commercially available silica gel (Cariact Q-50, Fuji Silysia Chemical Ltd.) which was 70 m²/g [90]. With these profits, it can propose that these prepared fibers can be used as the good adsorbents.

Moreover, the results of pore size distribution of all adsorbents including non-functionalization and functionalization with APTES were achieved by BJH theory in Figure 4.10 which shows the relation of pore volume (Y-axis) and pore diameter (X-axis). All contain the same characteristics of the pore size distribution and the most of pore diameters on their fibers of all adsorbents were 2.43 nm.

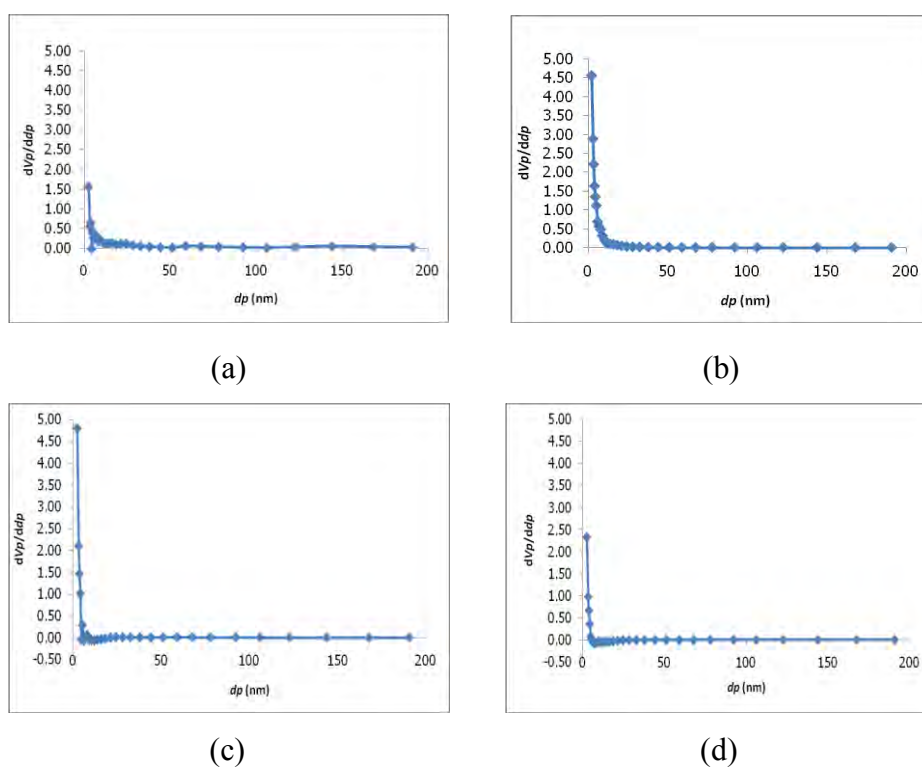


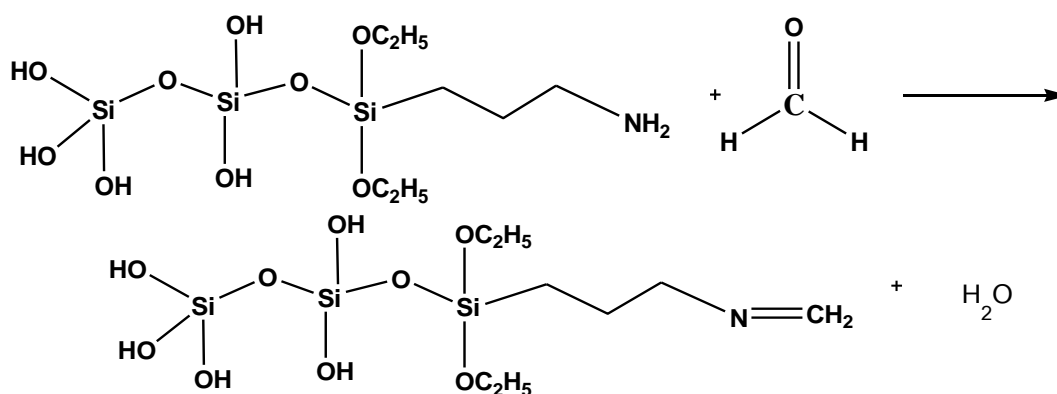
Figure 4.9 Pore size distribution of (a) non-functionalized and functionalized fibrous silica mats with (b) 0.15 M, (c) 0.50 M, (d) 1.00 M APTES, respectively

The pore sizes of all adsorbents were in the narrow range which was very low in nanometers (less than about 5 nm). From the nitrogen adsorption isotherm, and BET Plot, they resulted that the kind of pore diameters was mesoporosity which the size ranges between 2-50 nm and this also accords with the value of D_p in Table 4.8

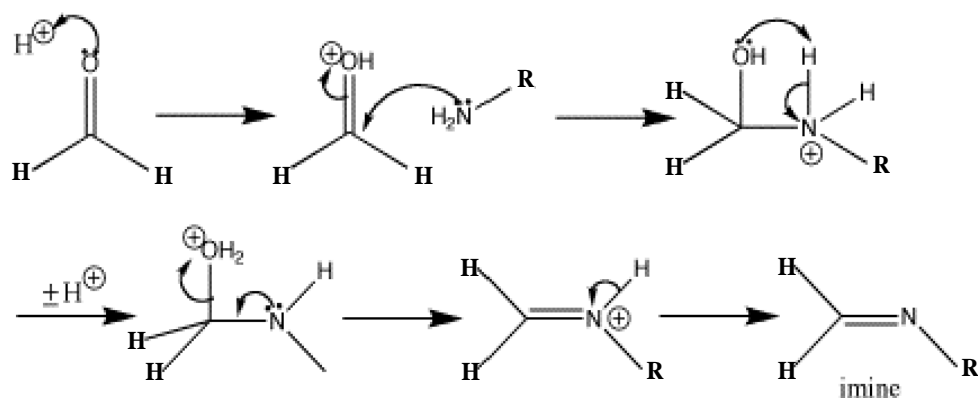
and corresponds to BJH theory shown in Figure 4.9. Therefore, it can conclude that all adsorbents are the mesoporous solids with the limited pore distribution about 2 nm.

4.3 Adsorption of formaldehyde in water

After the functionalization of electrospun fibrous silica mats with various APTES concentrations, the efficiency of functionalized silica fibers as adsorbents at optimum condition for formaldehyde adsorption in water was studied. Formaldehyde can be adsorbed on functionalized fibrous silica mats via chemical bonding at an amine group as shown in Scheme 4.4. The mechanism of reaction is presented in Scheme 4.5. An amine group grafted on silica surface (-NH_2) which is a strong nucleophile directly attach to a carbon atom of carbonyl group in formaldehyde structure to form ammonium ion. After that a proton of the quaternary ammonium transfers from the nitrogen to the negatively charged oxygen gives a neutral molecule. A proton from acid or dissociation of water protonates at hydroxyl group to form positively charged oxygen and water is then released. The lone pair on the amine comes to form double bond and push out water. The protonated imine and formaldehyde are the obtained products. At last, water molecule receives proton from the iminium ion ($\text{H}(\text{C}_3\text{H}_7)\text{N}^+=\text{CH}_2$) and imine ($\text{-N}=\text{CH}_2$) is formed.



Scheme 4.4 Reaction between functionalized silica fibers with APTES and formaldehyde (imine formation)



Scheme 4.5 The mechanism of reaction between APTES and formaldehyde (imine formation) where R represents $-\text{C}_3\text{H}_6\text{Si}(\text{OC}_2\text{H}_5)_3$ [91]

APTES concentrations for functionalization of fibrous silica mats and adsorption times are two main parameters for this study. Adsorbed quantity of formaldehyde with functionalized silica fibers at various APTES concentrations and adsorption times were shown in Figure 4.10 and Table 4.8.

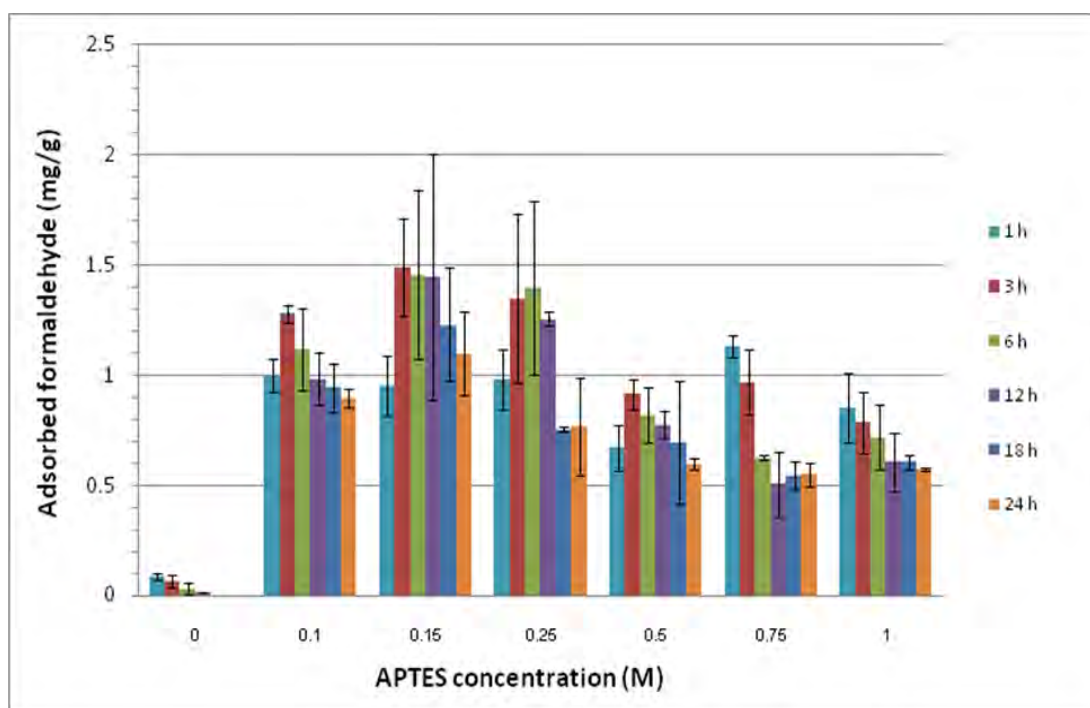
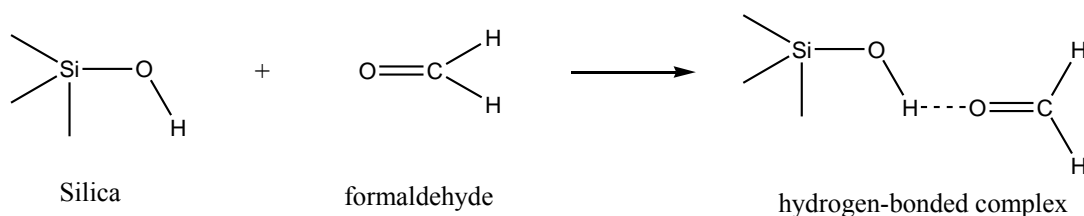


Figure 4.10 The relationship of APTES concentrations and adsorbed formaldehyde with functionalized silica fibers at various adsorption times

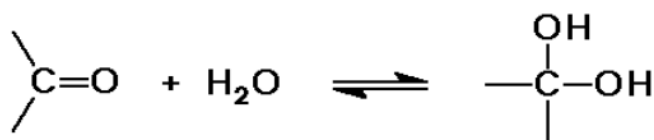
Table 4.8 Quantity of adsorbed formaldehyde with functionalized fibrous silica mats at various APTES concentrations and several adsorption times

APTES concentration (M)	Adsorbed formaldehyde (mg/g) at adsorption times of					
	1 hr	3 hrs	6 hrs	12 hrs	18 hrs	24 hrs
0.00	0.08±0.01	0.06±0.02	0.03±0.02	0.02±0.00	-	-
0.10	1.00±0.07	1.28±0.04	1.11±0.18	0.98±0.12	0.95±0.11	0.90±0.04
0.15	0.95±0.14	1.49±0.22	1.46±0.38	1.45±0.56	1.23±0.26	1.10±0.19
0.25	0.98±0.14	1.35±0.38	1.40±0.39	1.26±0.03	0.75±0.01	0.77±0.22
0.50	0.67±0.10	0.91±0.07	0.82±0.12	0.78±0.06	0.69±0.28	0.60±0.02
0.75	1.13±0.05	0.97±0.15	0.63±0.01	0.50±0.15	0.54±0.06	0.55±0.05
1.00	0.85±0.16	0.79±0.14	0.72±0.15	0.61±0.13	0.61±0.03	0.57±0.00

Adsorbed of formaldehyde with adsorbent indicates the efficiency of formaldehyde adsorption. If this value is high, it can assume that a kind of functionalized fibrous silica mat is an effective adsorbent. For non-functionalized electrospun fibrous silica mat, it was able to adsorb formaldehyde in water even though there is no aminopropyl group on the surface. However, its value was a lot lower than the functionalized fibrous silica mats. Yang and coworkers [14] had been reported that this was resulted from silanol group on the surface of non-functionalized silica fibers. It can form hydrogen bond with hydrogen atom of formaldehyde as presented in Scheme 4.6



Scheme 4.6 Chemical reaction between silica and formaldehyde [14]

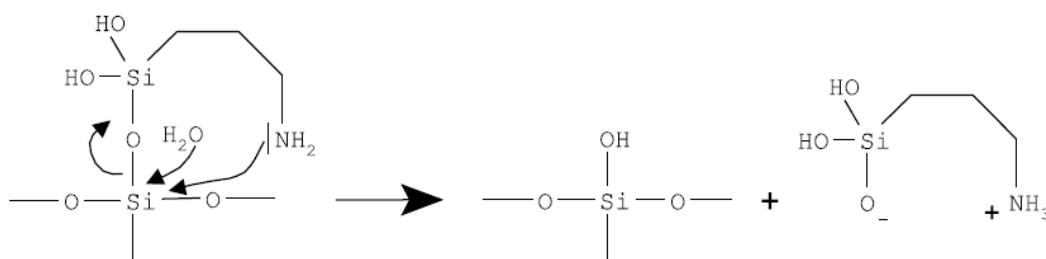


Scheme 4.7 Hydration reaction of aldehyde to form geminal diol

However, formaldehyde dissolving in water often forms a geminal diol with hydration reaction as in Scheme 4.7. This form can also react to silica with hydrogen bonding because of having two hydroxyl groups. As a result, non-functionalized silica fibers can slightly adsorb formaldehyde with very low amount in a short time (less than 3 hours).

From the graph in Figure 4.10, all functionalized fibrous silica mats showed the same trend of quantities of adsorbed formaldehyde. The adsorption efficiency was increased with the increment of adsorption time until 6 hours. After 6 hours (12-24 hrs), the quantity of adsorbed formaldehyde was decreased. This occurrence could describe that the amount of adsorptive sites were enough for adsorption during 1-6

hrs, so the amount of formaldehyde adsorption was increased. The capability of adsorption should be constant when the adsorbate (formaldehyde) was fully adsorbed on the limited sites of silica surface area and should not decrease when adsorption with a long time. However, after 6 hours, the quantity of adsorbed formaldehyde in all conditions was considerably decreased. This may be caused by the unstable of aminopropyl group on modified silica in aqueous solution and can leach in the external solution over prolonged periods of time (more than 1 hour) as shown in Scheme 4.8 [86]. Therefore, an immersing in aqueous solution with a long time could decrease the aminopropyl content on the silica surface, and resulting in a small reduction of the formaldehyde adsorption.



Scheme 4.8 Instability reaction of aminopropyl group on modified silica [86]

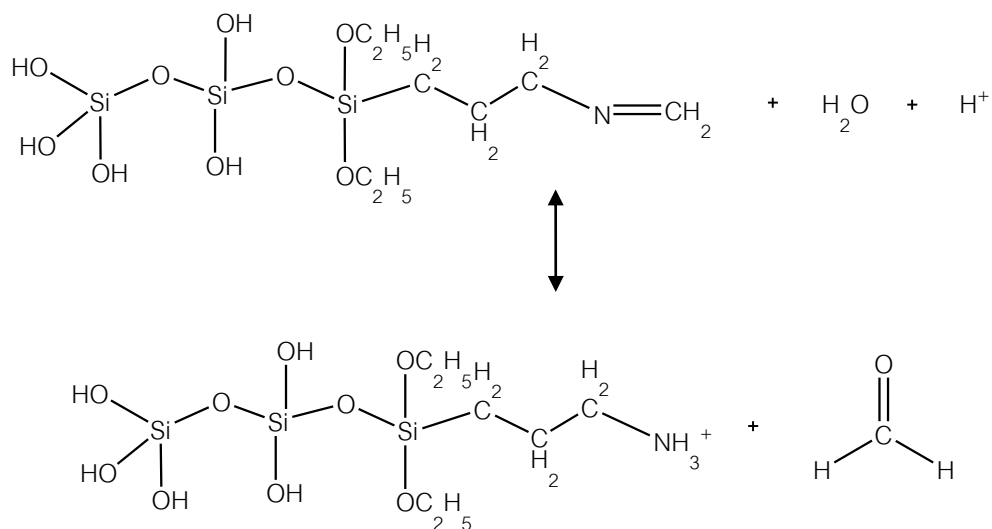
Basically, using the high concentration of APTES for silica modification should adsorb more than non-functionalized silica fibers and functionalized ones with lower APTES contents because a higher APTES content directly related to the increase in active sites on silica surface area and the capability of adsorption. Nevertheless, with high APTES content (0.50-1.00 M), the efficiency of these modified silica mats were low due to low surface area (from BET result) resulting from self-condensation of APTES becoming a bulk rather than fiber form (from SEM images). The functionalized fibrous silica mats with APTES concentration of 0.15 M and 0.25 M, could adsorb formaldehyde higher than 0.10 M APTES concentrations. Particularly, the functionalized silica fibers with 0.15 M APTES was considered as the most efficient adsorbent because it had higher specific surface area (from BET result) and sufficient adsorptive sites for adsorption higher aminopropyl loading as well as small reduction of quantity of adsorbed formaldehyde over a long period of adsorption time.

In observation of adsorption time, the quantity of adsorbed formaldehyde with functionalized silica with different APTES concentrations, especially at 0.10 M, 0.15 M, and 0.25 M APTES would increase in the time range of 3-12 hours and decrease when continuously adsorbed for 18-24 hours, but the fibrous silica mats which was functionalized with 0.50 M, 0.75 M, and 1.00 M APTES could increasingly adsorb in only short time range (< 3 hours) and decrease with more time (3-24 hours). It is possible causing from a high quantity of APTES on functionalized silica can only adsorb in the short-time range owing to abundant quantities of aminopropyl group and gradually decrease due to the reduction of the adsorptive sites and specific surface area. For lower APTES content of functionalized silica fibers (0.10 M-0.25 M), the efficiency of adsorption increased with a longer time range than high APTES content (0-6 hours) because formaldehyde was gradually adsorbed by a small content of APTES with higher specific surface area.

From the results, the concentration of APTES chosen for the optimized condition was 0.15 M because it gave a high adsorption efficiency, a higher surface area of adsorbent. And the adsorption time was selected for 3 hours because it was short, and offered a highly sufficient adsorption capacity although the quantity of adsorbed formaldehyde of adsorption for 6 hour was slightly more than of 3 hours.

4.4 Elution of adsorbed formaldehyde in water

The formaldehyde adsorption mechanism of functionalized fibrous silica mats with APTES was reversible. This reaction could return formaldehyde and form R-NH_3^+ by using acid as catalyst in aqueous solution as shown in Scheme 4.9. As a result, the amount of formaldehyde can then be determined or the reuse of fibrous silica mat is applicable.



Scheme 4.9 The regeneration of formaldehyde (the elution formaldehyde from aminopropyl functionalized silica)

Two kinds of acid including hydrochloric acid (HCl) and sulfuric acid (H₂SO₄) at various concentrations: 0.1 M, 0.3 M, 0.5 M, 1.0 M, 2.0 M, 3.0 M were used to elute the adsorbed formaldehyde.

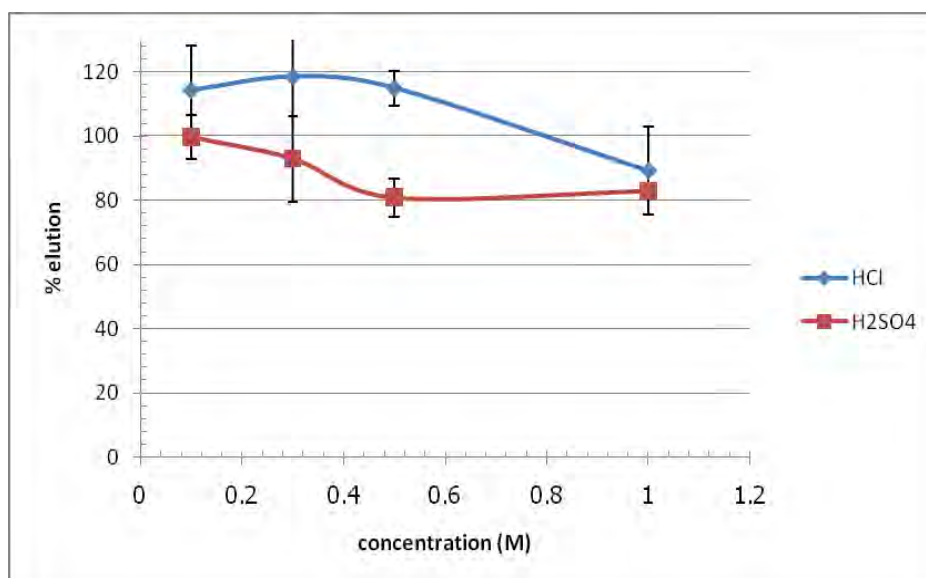


Figure 4.11 The relation between the percentage of elution and the various concentrations of HCl and H₂SO₄: 0.1, 0.3, 0.5, and 1.0 M at fixed time of 15 minutes

From the graph in Figure 4.11, both HCl and H₂SO₄ can elute formaldehyde about 80-120 %. The elution of formaldehyde with high concentration of acid (over than 1 M) was not determined because pH of solution was too low (1-2) and might not analyzed by the method used in this study. However, using both HCl and H₂SO₄ with low concentrations (about 0.1-1.0 M) was sufficient for elution and is not significantly different. Therefore, 0.1 M was selected as the optimum concentration of both HCl and H₂SO₄ used for elution.

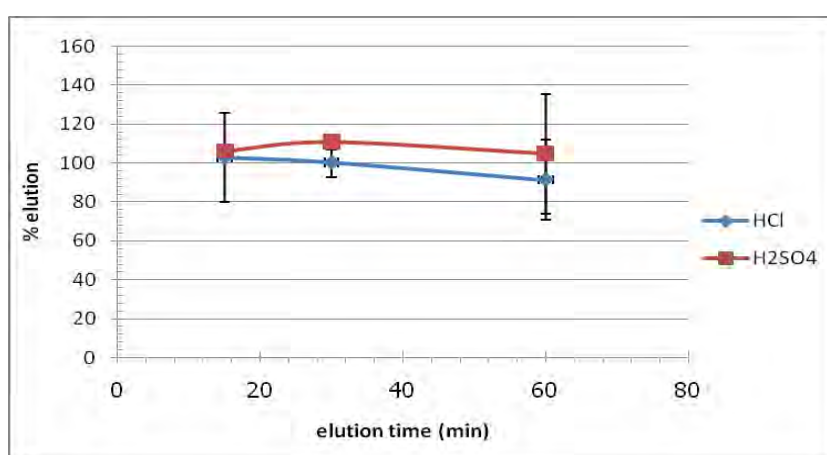


Figure 4.12 The relationship between elution time and the percentage of elution at the fixed concentration acid at 0.1 M.

Figure 4.12 presents the percentage of elution of formaldehyde at different times : 15, 30, 60 min using both HCl and H₂SO₄. The percentage of formaldehyde elution by both acids was almost equal (90-110%). Consequently, it may conclude that elution time does not affect the elution efficiency. Summarily, the elution with a short time (about 15 min) and low acid concentration (0.1 M) can be applied for any application.

CHAPTER V

CONCLUSION

5.1 Conclusion

From the synthesis via sol-gel process and fabrication with electrospinning, electrospun fibrous silica mats had been prosperously generated with the regular morphology and the diameters in the range of 200-270 nm. The factors of electrical potential and a distance between the collection screen and a syringe needle affected both the size and bead formation. The distance of 10 cm and the electrical potential 15 kV was selected as the optimum condition for electrospinning. Then, 3-aminopropyltriethoxysilane (APTES) was used as a silane coupling agent for functionalization of aminopropyl group on the silica fibers surface. The functionalized silica fibers with various APTES concentrations were characterized by Fourier-Transform infrared spectrometer (FT-IR), elemental analyzer (EA), thermogravimetric analyzer (TGA), surface area analyzer. The IR spectrum, EA and TGA indicated that aminopropyl group can be successfully grafted on electrospun fibrous silica mats and was in form of aminopropyl functionalized silica fibers. In addition, the results from scanning electron microscope (SEM) showed that the increase in APTES concentrations for functionalization led to dramatically change in the morphology of the fibers transformed into bulky solid. Moreover, the examination of the quantities of aminopropyl functionalized on the fibrous silica mats by EA and TGA resulted that the amount of aminopropyl grafted on the surface (loading capacity) were extended with the additional APTES contents. The results of Brunauer-Emmett-Teller (BET) surface area analyzer demonstrated that the surface area, pore volume and pore size distribution orderly decrease with increase in APTES contents.

In application in formaldehyde adsorption, functionalization silica fibers can adsorb formaldehyde with the same trend which increased in an early adsorption time (0-6 hour) and gradually decreased after 12 hours. The functionalized silica fibers

with small quantity of APTES (0.10-0.25 M) were more efficiently adsorb formaldehyde than the one with the higher quantity of APTES (0.5-1.0 M) because of the sufficient functional group for adsorption and the higher specific surface area. The optimum condition for adsorption was APTES concentration of 0.15 M with adsorption time of 3 hour. Lastly, the elution of adsorbed formaldehyde was studied. Both hydrochloric and sulfuric acid can be used for elution of formaldehyde with a good percentage. At the optimum condition for elution which is 0.1 M HCl or H₂SO₄ and the elution time of 15 minute, the percentage of elution was about 80-120%.

In conclusion, the functionalized electrospun fibrous silica mats with APTES was successfully prepared as a novel adsorbent for adsorption of formaldehyde in water.

5.2 Suggestion of future work

Because of low quantity of adsorbed formaldehyde (less than 1.5 mg/g), this experiment should be improved by pH adjustment of formaldehyde solution nearly be 4-6 which was the pH of imine formation and acid can work as catalyst of this reaction to form imine. This is an alternation for increasing of adsorption efficiency.

Although the novel adsorbent with good efficient adsorption was obtained, the development of this adsorbent in future may require. The functionalized silica fiber with amino group during sol-gel process is a challenge for development work. If this method can successfully generate, it will finely decrease the problem of the irregular distribution of aminopropyl group on silica fibers surface which may increase the efficiency of adsorbent for formaldehyde adsorption. Additionally, the preparation of formaldehyde sensor by functionalizing the colorimetric reagent on electrospun silica fibers surface which can adsorb formaldehyde and form the color when it reacts to formaldehyde is an alternative choice for future development.

REFERENCES

- [1] WHO, Formaldehyde. In Air Quality guidelines, 2 ed.; WHO Regional Office for Europe: pp 25. Copenhagen, Denmark: WHO Regional Office for Europe, 2001.
- [2] NPI. Formaldehyde (methyl aldehyde). Australia: Australian Government, Department of the Environment and Water Resources, April 2007.
- [3] ATSDR. Toxicological Profile for Formaldehyde (Draft). Atlanta, GA: Public Health Service, U.S. Department of Health and Human Services, 1997.
- [4] Liteplo, R. G.; Beauchamp, R.; Meek, M.E.; Chénier, R. Formaldehyde. Geneva: the United Nations Environment Programme, the International Labour Organization, and the World Health Organization, 2002:1-74.
- [5] Post, G. B. Formaldehyde Health-based maximum contaminant level. New Jersey: Office of Science and Research, New Jersey Department Environmental Protection.
- [6] McLaughlin, J. K. Formaldehyde and cancer: A critical review. International Archives of Occupational and Environmental Health 66 (1994): 295-301.
- [7] Feng, L.; Musto, C. J.; Suslick, K. S. A Simple and Highly Sensitive Colorimetric Detection Method for Gaseous Formaldehyde. Journal of the American Chemical Society 132: 4046-4047.
- [8] Boonamnuayvitaya, V.; Chaiya, C.; Tanthapanichakoon, W. The preparation and characterization of activated carbon from coffee residue. Journal of Chemical Engineering of Japan 37 (2004): 1504-1512.
- [9] Boonamnuayvitaya, V.; Sae-ung, S.; Tanthapanichakoon, W. Preparation of activated carbons from coffee residue for the adsorption of formaldehyde. Separation and Purification Technology 42 (2005): 159-168.
- [10] Kumagai, S.; Sasaki, K.; Shimizu, Y.; Takeda, K. Formaldehyde and acetaldehyde adsorption properties of heat-treated rice husks. Separation and Purification Technology 61 (2008): 398-403.
- [11] Takano, T.; Murakami, T.; Kamitakahara, H.; Nakatsubo, F. Formaldehyde adsorption by karamatsu (*Larix leptolepis*) bark. Journal of Wood Science 54 (2008): 332-336.

- [12] Tanada, S.; Kawasaki, N.; Nakamura, T.; Araki, M.; Isomura, M. Removal of formaldehyde by activated carbons containing amino groups. Journal of Colloid and Interface Science 214 (1999): 106-108.
- [13] Rong, H. Q.; Ryu, Z. Y.; Zheng, J. T.; Zhang, Y. L. Effect of air oxidation of Rayon-based activated carbon fibers on the adsorption behavior for formaldehyde. Carbon 40 (2002): 2291-2300.
- [14] Yang, H.; Weinstock, B. A.; Hirsche Ii, B. L.; Griffiths, P. R. Kinetic modeling of aldehyde adsorption rates on bare and aminopropylsilyl-modified silica gels by ultra-rapid-scanning fourier transform infrared spectrometry. Langmuir 21 (2005): 3921-3925.
- [15] Srisuda, S.; Virote, B. Adsorption of formaldehyde vapor by amine-functionalized mesoporous silica materials. Journal of Environmental Sciences 20 (2008): 379-384.
- [16] Jadkar, P. B.; Gupte, S. P.; Chaudhari, R. V. Adsorption of formaldehyde and butynediol from aqueous solutions on a Cu_2C_2 -silica gel catalyst. Reaction Kinetics and Catalysis Letters 27 (1985): 195-200.
- [17] Tsou, P. H.; Chou, C. K.; Saldana, S. M.; Hung, M. C.; Kameoka, J. The fabrication and testing of electrospun silica nanofiber membranes for the detection of proteins. Nanotechnology 19 (2008).
- [18] Choi, S. S.; Chu, B.; Lee, S. G.; Lee, S. W.; Im, S. S.; Kim, S. H.; Park, J. K. Titania-doped silica fibers prepared by electrospinning and sol-gel process. Journal of Sol-Gel Science and Technology 30 (2004): 215-221.
- [19] Choi, S. S.; Lee, S. G.; Im, S. S.; Kim, S. H.; Joo, Y. L. Silica nanofibers from electrospinning/sol-gel process. Journal of Materials Science Letters 22 (2003): 891-893.
- [20] Liu, Y.; Sagi, S.; Chandrasekar, R.; Zhang, L.; Hedin, N. E.; Fong, H. Preparation and characterization of electrospun SiO_2 nanofibers. Journal of Nanoscience and Nanotechnology 8 (2008): 1528-1536.
- [21] Kiba, N.; Sun, L.; Yokose, S.; Kazue, M. T.; Suzuki, T. T. Determination of nano-molar levels of formaldehyde in drinking water using flow-injection system with immobilized formaldehyde dehydrogenase after off-line solid-phase extraction. Analytica Chimica Acta 378 (1999): 169-175.

- [22] Kiba, N.; Yagi, R.; Sun, L. M.; Tachibana, M.; Tani, K.; Koizumi, H.; Suzuki, T. Poly(allylamine) beads as selective sorbent for preconcentration of formaldehyde and acetaldehyde in high-performance liquid chromatographic analysis. Journal of Chromatography A 886 (2000): 83-87.
- [23] Fang, J.; Niu, H.; Lin, T.; Wang, X. Applications of electrospun nanofibers. Chinese Science Bulletin 53 (2008): 2265-2286.
- [24] Huang, Z. M.; Zhang, Y. Z.; Kotaki, M.; Ramakrishna, S. A review on polymer nanofibers by electrospinning and their applications in nanocomposites. Composites Science and Technology 63 (2003): 2223-2253.
- [25] El-Nahhal, I. M.; El-Ashgar, N. M. A review on polysiloxane-immobilized ligand systems: Synthesis, characterization and applications. Journal of Organometallic Chemistry 692 (2007): 2861-2886.
- [26] Frondel, C. Systems of mineralogy Silica Minerals. 3, New York: John Wiley and Sons Inc., 1962.
- [27] Holleman, A. F., Wiberg, E. Inorganic Chemistry. San Diego: Academic Press, 2001.
- [28] Lager, G. A.; Jorgensen, J. D.; Rotella, F. J. Crystal structure and thermal expansion of α -quartz SiO_2 at low temperatures. Journal of Applied Physics 53 (1982): 6751-6756.
- [29] Wright, A. F.; Lehmann, M. S. The structure of β -quartz at 25 and 590°C determined by neutron diffraction. Journal of Solid State Chemistry 36 (1981): 371-380.
- [30] Downs, R. T.; Palmer, D. C. The pressure behavior of α -cristobalite. American Mineralogist 79 (1994): 9-14.
- [31] Wright, A. F., Leadbetter, A.J. The structures of the β -cristobalite phases of SiO_2 and AlPO_4 . Philosophical Magazine 31 (1975): 1391-1401.
- [32] Levien, L., Prewitt, C.T. High-pressure crystal structure and compressibility of coesite. American Mineralogist 66 (1981): 324-333.
- [33] Smyth, J. R., Swope, R.J., Pawley, A.R. H in rutile-type compounds: II. Crystal chemistry of Al substitution in H-bearing stishovite. American Mineralogist 80 (1995): 454-456.

- [34] Skinner, B. J., Appleman, D.E. Melanophlogite, a cubic polymorph of silica. American Mineralogist 48 (1963): 854-867.
- [35] Nakagawa, T., Kihara, K., Harada, K. The crystal structure of low melanophlogite. American Mineralogist 86 (2001): 1506.
- [36] Szostak, R. Molecular sieves: Principles of Synthesis and Identification. Springer, 1998.
- [37] Hriljac, J. A.; Eddy, M. M.; Cheetham, A. K.; Donohue, J. A.; Ray, G. J. Powder Neutron Diffraction and ²⁹Si MAS NMR Studies of Siliceous Zeolite-Y. Journal of Solid State Chemistry 106 (1993): 66-72.
- [38] Jal, P. K.; Patel, S.; Mishra, B. K. Chemical modification of silica surface by immobilization of functional groups for extractive concentration of metal ions. Talanta 62 (2004): 1005-1028.
- [39] Cadogan, D. F.; Sawyer, D. T. Gas-solid chromatography using various thermally activated and chemically modified silicas. Analytical Chemistry 42 (1970): 190-195.
- [40] Armistead, C. G.; Tyler, A. J.; Hambleton, F. H.; Mitchell, S. A.; Hockey, J. A. Surface hydroxylation of silica. The Journal of Physical Chemistry 73 (1969): 3947-3953.
- [41] Kiselev, A. V., Lygin, V.I. Infrared Spectra of Surface Compounds. New York: Wiley, 1975.
- [42] Ong, S.; Zhao, X.; Eisenthal, K. B. Polarization of water molecules at a charged interface: second harmonic studies of the silica/water interface. Chemical Physics Letters 191 (1992): 327-335.
- [43] Ceramic Abstracts. Journal of the American Ceramic Society 52 (1969): 303-334.
- [44] McCarthy, G. J.; Roy, R.; McKay, J. M. Preliminary Study of Low-Temperature "Glass" Fabrication from Noncrystalline Silicas. Journal of the American Ceramic Society 54 (1971): 637-638.
- [45] Iler, R. K. The Chemistry of Silica. New York: Wiley, 1955.
- [46] Stober, W.; Fink, A.; Bohn, E. Controlled growth of monodisperse silica spheres in the micron size range. Journal of Colloid and Interface Science 26 (1968): 62-69.

- [47] Davis, J. T., Rideal, E. K. In Interfacial Phenomena. New York: Academic Press, 1963.
- [48] Flory, P. J. Principle of Polymer Chemistry. Ithaca, NY: Cornell University Press, 1953.
- [49] Branda, F.; Silvestri, B.; Luciani, G.; Costantini, A. The effect of mixing alkoxides on the Stober particles size. Colloids and Surfaces A: Physicochemical and Engineering Aspects 299 (2007): 252-255.
- [50] Ketelson, H. A.; Pelton, R.; Brook, M. A. Surface and colloidal properties of hydrosilane-modified Stober silica. Colloids and Surfaces A: Physicochemical and Engineering Aspects 132 (1998): 229-239.
- [51] Liu, S.; Lu, L.; Yang, Z.; Cool, P.; Vansant, E. F. Further investigations on the modified Stober method for spherical MCM-41. Materials Chemistry and Physics 97 (2006): 203-206.
- [52] Hench, L. L.; West, J. K. The sol-gel process. Chemical Reviews 90 (1990): 33-72.
- [53] Lev, O.; Tsionsky, M.; Rabinovich, L.; Glezer, V.; Sampath, S.; Pankratov, I.; Gun, J. Organically modified sol-gel sensors. Analytical Chemistry 67 (1995): 22A-30A.
- [54] Pyell, U.; Stork, G. Preparation and properties of an 8-hydroxyquinoline silica gel, synthesized via mannich reaction. Fresenius' Journal of Analytical Chemistry 342 (1992): 281-286.
- [55] Colli, M.; Gironi, A.; Molina, V.; Marchetti, R.; Melzi D'Eril, G.; Lucarelli, C. Improved HPLC methodology in occupational exposure studies on formaldehyde. Chromatographia 32 (1991): 113-115.
- [56] Mahmoud, M. E. Silica gel-immobilized Eriochrome black-T as a potential solid phase extractor for zinc (II) and magnesium (II) from calcium (II). Talanta 45 (1997): 309-315.
- [57] Prado, A. G. S.; Airoidi, C. Adsorption, preconcentration and separation of cations on silica gel chemically modified with the herbicide 2,4-dichlorophenoxyacetic acid. Analytica Chimica Acta 432 (2001): 201-211.
- [58] Soliman, E. M.; Mahmoud, M. E.; Ahmed, S. A. Synthesis, characterization and structure effects on selectivity properties of silica gel covalently bonded

diethylenetriamine mono- and bis-salicylaldehyde and naphthaldehyde Schiff's bases towards some heavy metal ions. Talanta 54 (2001): 243-248, 250-253.

[59] Zhang, X.; Wu, W.; Wang, J.; Tian, X. Direct synthesis and characterization of highly ordered functional mesoporous silica thin films with high amino-groups content. Applied Surface Science 254 (2008): 2893-2899.

[60] Zeleny, J. The electrical discharge from liquid points, and a hydrostatic method of measuring the electric intensity at their surfaces. Physical Review 3 (1914): 69-91.

[61] Huang, Z. M., Zhang, Y. Z., Kotaki, M., Ramakrishna, S. A review on polymer nanofibers by electrospinning and their applications in nanocomposites. Composites Science and Technology 63 (2003): 2223-22253.

[62] Vonnegut, B., Newbauer, R.I. Production of monodisperse liquid particles by electrical atomization. Journal of Colloid and Interface Science 7 (1952): 616-622.

[63] Simons, H. L. Process and Apparatus for Producing Patterned Nonwoven Fabrics. 3 (1966): 229.

[64] Taylor, G. I. In Electrically Driven Jets, The Royal Society of London. Proceedings. Series A. Mathematical, Physical and Engineering Sciences., London, pp 453-475. London, (1934-1990), 1969.

[65] Sill, T. J.; von Recum, H. A. Electrospinning: Applications in drug delivery and tissue engineering. Biomaterials 29 (2008): 1989-2006.

[66] Baumgarten, P. K. Electrostatic spinning of acrylic microfibers. Journal of Colloid and Interface Science 36 (1971): 71-79.

[67] Larrondo, L.; St. John Manley, R., Electrostatic fiber spinning from polymer melts. III. Electrostatic deformation of a pendant drop of polymer melt. John Wiley & Sons, Inc.: 1981; Vol. 19, pp 933-940.

[68] Bhardwaj, N.; Kundu, S. C. Electrospinning: A fascinating fiber fabrication technique. Biotechnology Advances 28 (2010): 325-347.

[69] Rutledge, G. C.; Fridrikh, S. V. Formation of fibers by electrospinning. Advanced Drug Delivery Reviews 59 (2007): 1384-1391.

[70] Kim, K.; Turnbull, R. J. Generation of charged drops of insulating liquids by electrostatic spraying. Journal of Applied Physics 47 (1976): 1964-1969.

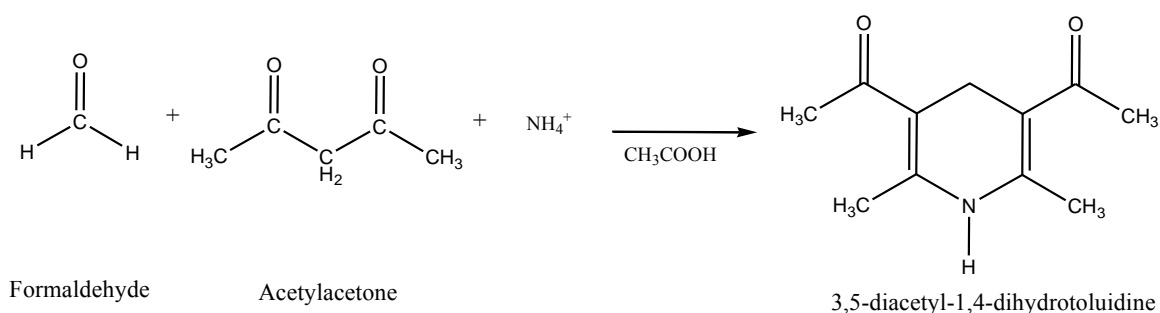
- [71] Andradý, A. L. Science and Technology of Polymer Nanofibers. Canada: John Wiley & Sons, Inc., 2008. p 403.
- [72] Saville, D. A. Electrohydrodynamic Stability: Fluid Cylinders in Longitudinal Electric Fields. Physics of Fluids 13 (1970): 2987-2994.
- [73] Saville, D. A. Stability of Electrically Charged Viscous Cylinders. Physics of Fluids 14 (1971): 1095-1099.
- [74] Reneker, D. H.; Yarin, A. L.; Fong, H.; Koombhongse, S. Bending instability of electrically charged liquid jets of polymer solutions in electrospinning. Journal of Applied Physics 87 (2000): 4531-4547.
- [75] Haghi, A. K.; Akbari, M. Trends in electrospinning of natural nanofibers. Physica Status Solidi (a) 204 (2007): 1830-1834.
- [76] Hohman, M. M.; Shin, M.; Rutledge, G.; Brenner, M. P. Electrospinning and electrically forced jets. I. Stability theory. Physics of Fluids 13 (2001): 2201-2220.
- [77] Hohman, M. M.; Shin, M.; Rutledge, G.; Brenner, M. P. Electrospinning and electrically forced jets. II. Applications. Physics of Fluids 13 (2001): 2221-2236.
- [78] Wang, X.; Um, I. C.; Fang, D.; Okamoto, A.; Hsiao, B. S.; Chu, B. Formation of water-resistant hyaluronic acid nanofibers by blowing-assisted electro-spinning and non-toxic post treatments. Polymer 46 (2005): 4853-4867.
- [79] Sudaray, B., Subramanian, V., Natarajan, T.S., Xiang, R.Z., Chang C.C., Fann, W.S. Electrospinning of continuous aligned polymer fibers. Applied Physics Letters 84 (2004): 1222-1224.
- [80] Li, D., Xia, Y. Electrospinning of nanofibers: reinventing the wheel. Advanced Materials 16 (2004): 1151-1170.
- [81] Xu, C. Y., Inai, R., Kotaki, M., Ramakrishna, S. Aligned biodegradable nanofibrous structure: a potential scaffold for blood vessel engineering. Biomaterials 25 (2004): 877-886.
- [82] Sing, K. S. W. Physisorption of nitrogen by porous materials. Journal of Porous Materials 2 (1995): 5-8.
- [83] Sing, K. S. W., Everett, D. H. E.; Haul, R.A.W., Moscou, L.; Siemieniewska, T. Reporting Physisorption Data For Gas/Solid Systems with Special Reference to the Determination of Surface Area and Porosity. 57, Great Britain: IUPAC, 1985. p 603-619.

- [84] Aligizaki, K. K. Pore structure of cement-based materials : testing, interpretation and requirements. Abingdon: Taylor & Francis, 2005. p 388.
- [85] Zeleňák, V.; Badaničová, M.; Halamová, D.; Čejka, J.; Zukal, A.; Murafa, N.; Goerigk, G. Amine-modified ordered mesoporous silica: Effect of pore size on carbon dioxide capture. Chemical Engineering Journal 144 (2008): 336-342.
- [86] Etienne, M.; Walcarius, A. Analytical investigation of the chemical reactivity and stability of aminopropyl-grafted silica in aqueous medium. Talanta 59 (2003): 1173-1188.
- [87] Imyim, A.; Prapalimrungsi, E. Humic acids removal from water by aminopropyl functionalized rice husk ash. Journal of Hazardous Materials Article In Press, doi:10.1016/j.jhazmat.2010.08.108
- [88] Bois, L.; Bonhommé, A.; Ribes, A.; Pais, B.; Raffin G.; Tessier, F. Functionalized silica for heavy metal ions adsorption. Colloids and Surfaces A: Physicochemical and Engineering Aspects 221 (2003) 221-230.
- [89] Wang, X.; Jin Ma; Jin Liu; Zhou, C.; Shouzhi Yi, Y.Z.; Yang, Z. Hierarchically mesoporous silica materials prepared from the uniaxially stretched polypropylene membrane and surfactant templates. Nanotechnology 17 (2006): 3627.
- [90] Tsubaki, N.; Zhang, Y.; Sun, S.; Mori, H.; Yoneyama, Y.; Li, X.; Fujimoto, K. A new method of bimodal support preparation and its application in Fischer-Tropsch synthesis. Catalysis Communications 2 (2001): 311-315.
- [91] Shaughnessy, K. Imine formation.[online]. Chem 232 Spring 2010. 2009. Available from:
<http://bama.ua.edu/~kshaughn/chem232/resources/mechanisms/review/imine/imine1.htm> [2009, 21 September].

APPENDIX

Detection of formaldehyde by ASTM method [D6303-98]

Quantities of formaldehyde solution after adsorption or elution were detected as absorbance value at maximum wavelength 412 nm by UV-visible spectrophotometer. Prior to detection, formaldehyde solution needed to be derivatized by acetyl acetone reagent consisted of 15.4 g ammonium acetate, 200 μ L acetyl acetone and 300 μ L glacial acetic acid in 100 mL deionized water. And then the resultant yellow solutions were heated at 60°C for 10 minutes. When the solutions were cooled down to room temperature, these were ready to detect with the above mention technique. The reaction is shown following as :



Scheme A-1 Derivatization of formaldehyde to form 3,5-diacetyl-1,4-dihydroxylidine

Eight standard formaldehyde solutions including concentrations of 0.0, 0.5, 1.5, 2.5, 3.5, 4.5, 6.0, and 7.5 ppm were prepared for calibration curve by dilution of 10 ppm HCHO solution that was prepared from 1000 ppm formaldehyde stock solution. And formaldehyde samples which obtained from adsorption and elution for detection with the spectrometer must be diluted until concentrations of these are in the linear range of calibration curve.

VITA

Miss Unchalee Thuambangphai was born on May 9, 1985 in Bangkok, Thailand. She graduated with a Bachelor of Science degree in Chulalongkorn University in 2006. After that, she has been a graduated student at the Department of Chemistry Chulalongkorn University and become a member of Chromatography and Separation Research Unit. She finished her Master's degree of Science in 2010.